Investigating the role of NADPH oxidases during infection related development of the rice blast fungus *Magnaporthe oryzae*

Submitted by Olivia Goode

to the University of Exeter as a dissertation for the degree of Masters by Research, in Biological Sciences.

January 2018

I certify that all material in this dissertation which is not my own work has been identified and that no material has previously been submitted and approved for the award of a degree by this or any other University.

Olivia Goode

Abstract

Rice blast disease is a major threat to global food security, destroying 30% of annual rice crops globally, and with disease remaining difficult to control. The causal agent of rice blast, *Magnaporthe oryzae* infects plants with a specialised single-celled infection structure called an appressorium, which accumulates glycerol to develop enormous intracellular turgor, using osmotic pressure to drive a rigid penetration peg through the rice leaf cuticle. NADPH oxidases (Nox) are flavoenzymes that function by transferring electrons across biological membranes to catalyse the reduction of molecular oxygen to superoxide. In filamentous fungi, Nox are necessary for cellular differentiation associated with sexual reproduction and host tissue invasion, such as processes involving the transition of cell growth from non-polarized growth to polarized growth. Previously, in *M. oryzae* it has been shown that Nox are essential for septin-mediated re-orientation of the F-actin cytoskeleton to facilitate penetration peg formation and plant cell invasion. The mechanism of assembly and activation of the Nox complex at the plasma membrane in *M. oryzae* is still unknown. Here I show the assembly of the Nox complex by determining the physical interactions of putative Nox associated proteins using yeast two-hybrid analysis and models of these interactions are presented. Yeast two-hybrid analysis revealed evidence of interactions between putative Nox components and the cytoskeleton element Chm1, which suggests the Nox complex may have a role in cytoskeleton remodeling during penetration peg formation. Analysis also revealed a potential scaffold protein for the recruitment of soluble proteins to the membrane bound Nox complex, Bem1, as the protein interacted with all putative Nox components investigated. In addition I generated a *Δpls1* mutant using a one-step gene replacement procedure. I confirmed that the mutant is unable to cause rice blast disease.

Table of Contents

Abbreviations

CM, complete medium; EDTA, ethylenediaminetetraacetic acid; TBE, Tris/Borate/EDTA; YPDA, yeast peptone dextrose adenine; YPD, yeast peptone dextrose; TE, Tris/EDTA; LiAc; Lithium acetate; SD, synthetic defined; OCM, osmotically controlled medium; CTAB, hexadecyltrimethylammonium bromide; °C, degrees Celsius; DNA, deoxyribonucleic acid; GFP, green fluorescent protein; g, grams; L, litre; µg, microgram; mM, millimolar; M, molar; cDNA, complementary deoxyribonucleic acid; ORF, open reading frame; PCR, polymerase chain reaction; ROS, reactive oxygen species; WT, wild-type; hpi, hours post infection; AD, activation domain; BD, binding domain; MCR, multiple cloning region.

List of Tables and Figures

Figure 4.1 Proposed model depicting the Nox1 and Nox2 complex using yeast two-hybrid data.

1. Introduction

1.1 Food security and rice blast disease

The protection of crops from disease is essential to safeguard global food security, especially with the expanding global population estimated to reach 9.8 billion by 2050 (United Nations, 2017). The inequality between food production with distribution and demand leaves an estimated 800 million people undernourished, mainly found in underdeveloped countries with high levels of poverty (Skamnioti & Gurr, 2009; Strange & Scott, 2005). Increasing food production by reducing crop destruction by plant pathogens is a major element in combating malnutrition, as it is estimated that plant pathogens reduce global food production by 10% (Strange & Scott, 2005).

One of the most important staple crops globally is rice (*Oryza sativa*) which provides 23% of the world's calories (Osés Ruiz & Talbot, 2017). Rice is a widely grown crop with 700 million tonnes produced each year, 92% grown and consumed in Asia where it is the most important food product (Osés Ruiz & Talbot, 2017; Wilson & Talbot, 2009). It is estimated that 30% of the rice harvest is lost every year due to rice blast disease, which is caused by the ascomycete fungus *Magnaporthe oryzae* (Talbot, 2003). The disease, originally called 'rice fever disease' as it spreads rapidly through fields, has been described since the 17th century and first reported in China (Couch et al., 2005).

M. oryzae infects all aerial parts of the rice plant including leaves, stems, nodes and panicles at all stages of development (**Figure 1.1**) (Wilson & Talbot, 2009). If the panicle infection occurs this can lead to total loss of grain (R. Dean et al., 2012).

Figure 1.1 Rice blast disease lesions on rice.

Foliar infection of a rice plant by *M. oryzae* causing leaf spot disease characterised by large, spreading lesions with a necrotic centre and chlorotic margin. Adapted from Wilson & Talbot, 2009.

Controlling plant pathogens has proven difficult because of the increase in transportation of crops globally, the reduced genetic variation of monocultures leaving them susceptible to non-native plant pathogens and the high genetic variation of pathogens in the field (Skamnioti & Gurr, 2009). Control measures to tackle rice blast include avoiding excess use of nitrogen-based fertilisers, planting disease-free seed, growing with high soil moisture such as under continuous flooding, planting blast-resistant cultivars and using fungicides (Seebold et al., 2004; Skamnioti & Gurr, 2009). Fungicides are the most effective control method however, the high cost and labour-intensive application mean many farmers do not use them (Seebold et al., 2004). Disease resistant cultivars can provide resistance however, these typically only last 2-3 growing seasons before the fungus is able to overcome new resistant traits (Wilson & Talbot, 2009).

M. oryzae is found globally and is able to infect other economically important crops such as: wheat, barley, finger millet, oats and rye grass (Talbot, 2003). Wheat blast disease is an emerging disease which was first identified in Brazil in 1985 (Kohli et al., 2010). In February 2016, an outbreak of wheat blast was identified in eight districts of Bangladesh, this is the first time wheat blast has

been detected in Asia (Islam et al., 2016). Using phylogenetic analysis the lineage of the wheat blast fungus was found to originate from South America (Islam et al., 2016). This epidemic caused a loss of 15,000 hectares of crops that affected 15% of the cultivated wheat fields in the infected eight districts of Bangladesh (Callaway, 2016). Fields were burnt as a low cost method to stop the spread of the disease into neighbouring India. However in March 2017, *M. oryzae* was found in West Bengal, India (Das, 2017). Similar to Bangladesh, the crops and seeds were destroyed to stop the disease disseminating further into India (Bhattacharya & Mondal, 2017). This economically impacted the farmers as the loss they sustained was not equivalent to the compensation they received due to the preventative measures (Bhattacharya & Mondal, 2017).

1.2 The Lifecycle of *M. oryzae*

M. oryzae is a hemi-biotrophic ascomycete fungus, which is able to infect the stem, leaves, nodes, panicles and roots of rice plants (Wilson & Talbot, 2009). The lifecycle, shown in **Figure 1.2**, starts with a three celled conidium landing on a hydrophobic rice leaf for foliar infection. To prevent the conidium from being dislodged by environmental conditions, the apical compartment secretes spore tip mucilage, an adhesive to stick to the surface of the leaf (Hamer et al., 1988).

Germination occurs in the presence of water to produce a narrow polarised germ tube which grows across the leaf cuticle (Bourett & Howard, 1990). The germ tube apex hooks and swells to differentiate into an incipient appressorium, a dome shaped single cell infection structure (Bourett & Howard, 1990; Talbot, 2003). The appressorium will only form on a hard hydrophobic surface and induced by environmental cues such as surface hardness, hydrophobicity and cutin monomers (R. A. Dean, 1997; Martin-urdiroz et al., 2015). During appressorium formation a mitotic event occurs in the conidium and one daughter

nuclei travels down the germ tube toward the appressorium (Bourett & Howard, 1990). Appressorium differentiation and maturation requires two S-phase checkpoints to be fulfilled before progression (Osés Ruiz & Talbot, 2017). The conidium collapses requiring autophagy where the spore contents is transferred to the maturing appressorium (Kershaw & Talbot, 2009). As the appressorium matures a melanin layer forms between the chitin rich cell wall and cell membrane which prevents the efflux of solutes. (R. A. Dean, 1997). The high concentration of glycerol leads to an influx of water by diffusion resulting in the swelling of the cell allowing up to 8 MPa of turgor to be produced (de Jong et al., 1997; Howard et al., 1991). To puncture the leaf cuticle turgor pressure is translated into mechanical force where a narrow penetration peg emerges from the base of the appressorium, breaching the rice leaf cuticle to cause disease (Ebbole, 2007).

The emergence of the penetration peg requires cytoskeleton remodelling at the appressorial pore to re-establish polarised growth (Dagdas et al., 2012). During turgor generation a toroidal F-actin ring is formed around the appressorium pore (Dagdas et al., 2012). Re-organisation of the F-actin requires septin guanosine triphosphates (GTPases) to form a hetero-oligomeric ring which is known to scaffold actin (Dagdas et al., 2012). The septin ring is phosphorylated by Chm1 proteins also organised into a ring network (Ryder et al., 2013). The septin ring acts as a diffusion barrier to localise membrane curvature proteins including Bin-Amphiphysin-RVS (BAR)-domain proteins and a WASP/Arp2/3 complex component, Las17 (**Figure 1.3**) (Dagdas et al., 2012). The pressure pushes the rigid penetration peg through the leaf cuticle and a primary invasive hyphae is produced to colonise the first cell. The invasive hyphae grow in a branched and bulbous form that invaginate the plant plasma membrane in the first occupied

epidermal cell, before moving into neighbouring cells via pit fields and plasmodesmata (Kankanala et al., 2007; Yan & Talbot, 2016)

A necrotic disease lesion appears after three days on the surface of the leaf and after five days under high humidity sporulation occurs (Talbot, 2003). Each lesion is able to produce 20,000 spores per night for 20 days which are spread to the next host by aerial and dewdrop dispersion to compete the cycle (Talbot, 2003).

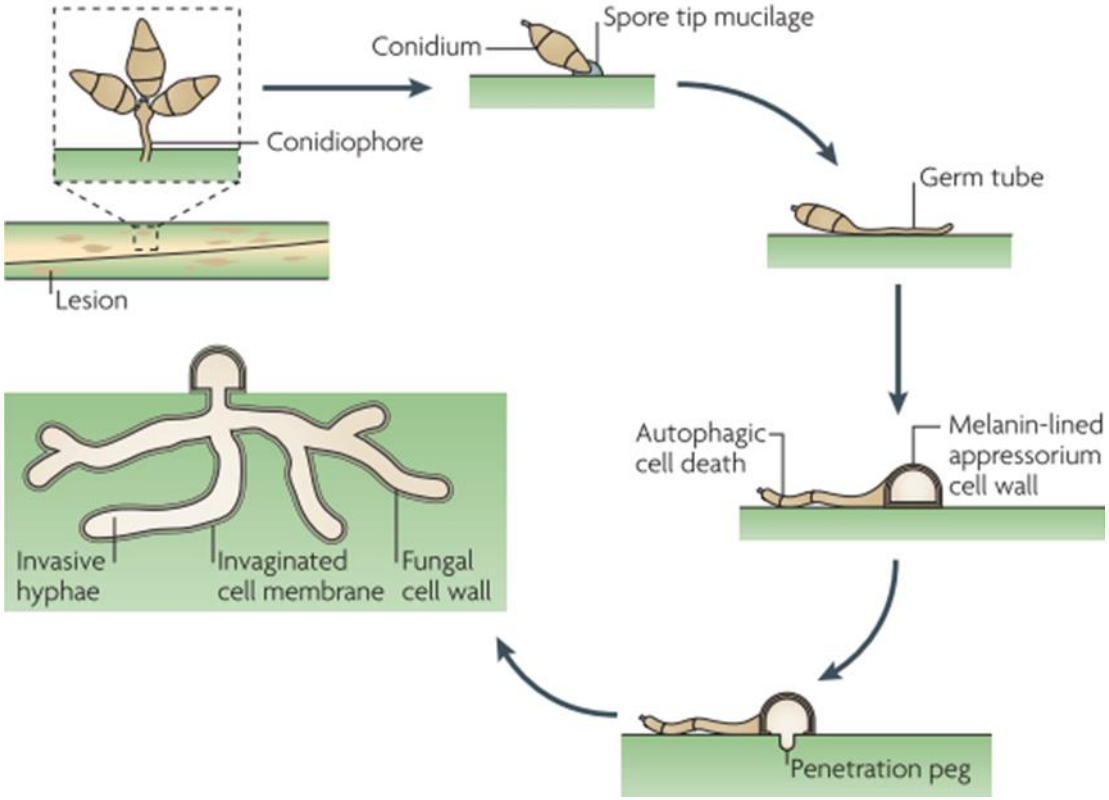

Figure 1.2 The life cycle of *Magnaporthe oryzae*.

A three cell conidium lands on a hydrophobic rice leaf surface and attaches using spore tip mucilage. The conidium germinates to produce a narrow germ tube which differentiates at the tip to form an appressorium. The appressorium matures, forming a melanin-lined cell wall and the conidium collapses. The appressorium produces turgor pressure which is translated into mechanical force to form a penetration peg, penetrating the leaf cuticle. An invasive hyphae enters the cell and branched hyphae are produced to colonise the cell, moving cell to cell via pit fields. After 72 hours a disease lesion can be seen and sporulation occurs to complete the cycle. Reprinted from Wilson & Talbot, 2009.

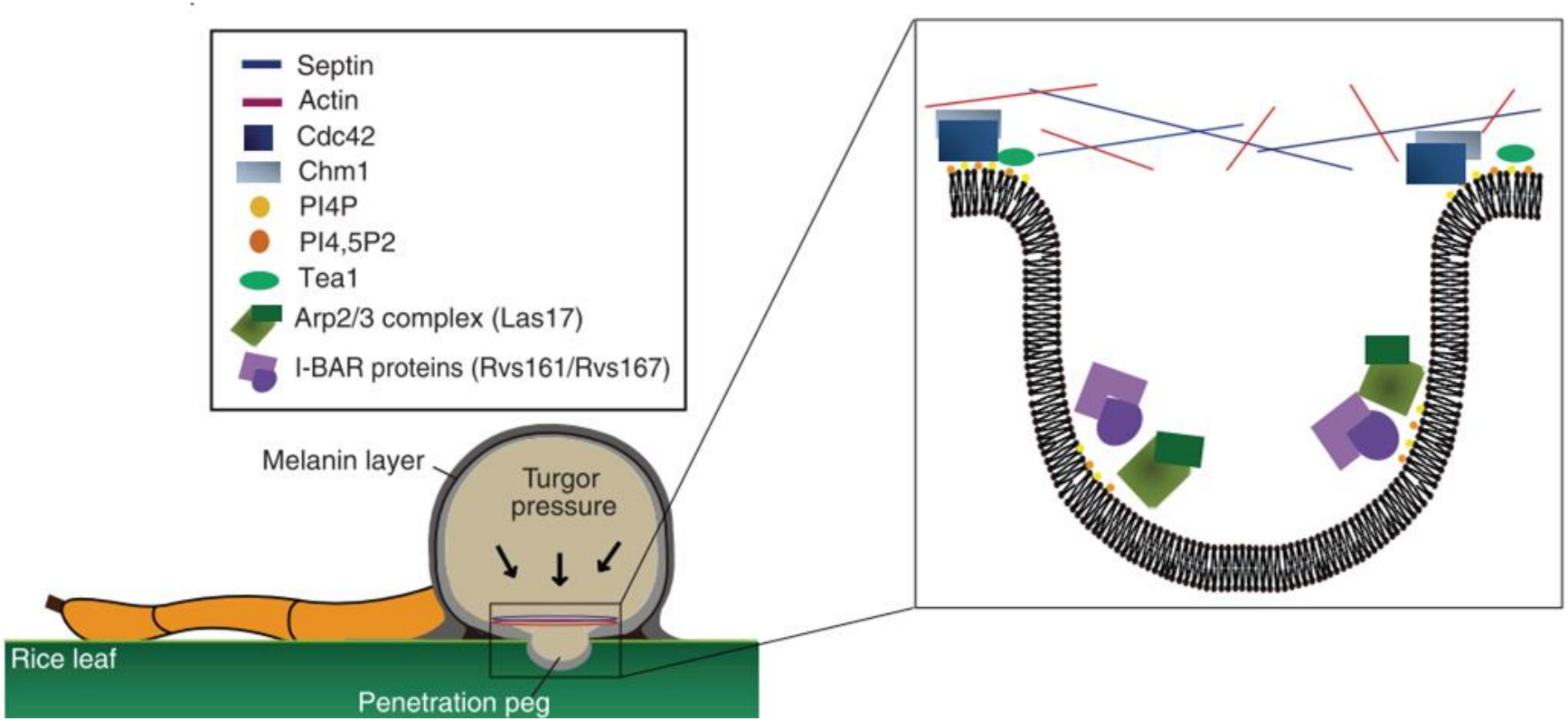

Figure 1.3 A model of septin-mediated penetration peg formation in *M. oryzae* during plant infection.

During appressorium maturation localisation of specific proteins to the appressorium pore allow membrane curvature and penetration peg emergence. Chm1 kinase phosphorylates septins to form a ring at the appressorium pore which acts as a scaffold for an F-actin toroidal network initiating polarised growth. The septin ring forms a diffusion barrier to allow the concentration of membrane curvature proteins (Arp2/3 complex, I-BAR proteins). Reprinted from Dagdas et al., 2012.

1.3 NADPH oxidases and Nox

NADPH oxidases (Nox) are flavoenzymes which generate reactive oxygen species (ROS) by catalysing the conversion of molecular oxygen to superoxide (Lambeth, 2004). Nox enzymes are associated with a diverse range of different cellular processes however, the precise role of these enzymes remains unclear. In eukaryotic cells Nox enzymes are involved in cellular differentiation, cellular proliferation, cellular signalling, apoptosis and the switch between non-polarised and polarised growth (Ryder et al., 2013; Takemoto et al., 2011). In plants however they are involved in polarised growth of root hairs, pathogen infection, programmed cell death and in response to environmental stressors (Foreman et al., 2003; Suzuki et al., 2011; Torres et al., 2002).

The best characterised Nox complex is found during phagocytosis in the vacuoles of human phagocytes (Segal & Jones, 1978). The complex consists of a membrane-bound catalytic component gp91phox and regulatory subunits p22phox, p47phox, p40phox, p67phox and a small GTPase RAC, which when assembled forms the active complex (Lam et al., 2010; Lambeth, 2004). The Nox complex is used to catalyse the respiratory burst in the defence response which involves the consumption of oxygen to produce ROS (Baldridge & Gerard, 1933; Lambeth, 2004). The respiratory burst was first hypothesised to be a mitochondrial response, however later studies found that the burst was unaffected by inhibitors of mitochondrial oxidative metabolism such as cyanide and antimycin A (Cross & Segal, 2004; Sbarra & Karnovskyi, 1959). They play a critical role in host immunity as patients with the genetic disease chronic granulomatous disease (CGD), characterised by recurrent and severe bacterial and fungal infections, are associated with defective NOX2 activity (Holmes et al., 1967; Segal, 2005). During phagocytosis the multi-component Nox complex is

activated once the vacuole has closed and is responsible for producing a Nox-dependent oxidative burst (Lambeth, 2004). This produces a high concentration of ROS, and with the change in the pH of the phagocytic vacuole leads to the destruction of the pathogen by the activation of proteases (Cross & Segal, 2004; Reeves et al., 2002).

In filamentous fungi, ROS is not used in a defence response but implicated in cell signalling (Ryder et al., 2013). Three Nox enzymes have been characterised, Nox1 (NoxA) and Nox2 (NoxB) which are homologues of $gp91^{phox}$ and Nox3 (NoxC) which has putative calcium binding EF-hand motifs (Tudzynski et al., 2012). Deletion of *NOXA* in *Aspergillus nidulans, Podospora anserina* and *Neurospora crassa* indicated NoxA is required for the development of sexual fruiting bodies (Cano-Domínguez et al., 2008; Lara-Ortíz et al., 2003; Malagnac et al., 2004). NoxA also has a role implicated in the chitin biosynthesis and strengthening of the cell wall by oxidative crosslinking (Egan et al., 2007). Deletion of *NOXB* affects ascospore germination in *N. crassa and P. anserina* (Cano-Domínguez et al., 2008; Malagnac et al., 2004). Compared to the other Nox complexes NoxC is only found in 7 ascomycota fungi and the function remains less understood (Takemoto et al., 2007).

In *M.* oryzae the oxidative burst generated by Nox1 and Nox2 is required for plant infection and if either gene is disrupted the resulting mutant is non-pathogenic (Clergeot et al., 2001; Ryder et al., 2013). During penetration peg formation the F-actin cytoskeleton undergoes remodelling, this is a Nox1 and Nox2 dependent process and deletion of either Nox1 or Nox2 results in a disorganised F-actin network (Ryder et al., 2013). Nox1 plays a role in the extension of the penetration peg and the deletion of the gene results in formation of a penetration peg with a disorganised F-actin network, which is unable to elongate to puncture the leaf cell

wall to colonise the host (Ryder et al., 2013). Unlike *Δnox1* mutants, deletion of *NOX2* prevents formation of a penetration peg (Ryder et al., 2013). *Δnox2* mutants have a disorganised septin and Chm1 ring, as well as a disorganised F-actin network meaning there is no diffusion barrier to concentrate membrane curvature proteins for formation of the penetration peg (Ryder et al., 2013). This evidence suggests that the Nox1 and Nox2 dependent oxidative burst is required for the formation and elongation of the penetration peg, allowing the pathogen to puncture the leaf cell below to cause infection.

Previous studies have suggested that *PLS1* is associated with Nox2 activity in *M. oryzae* (Ryder et al., 2013; Tudzynski et al., 2012). Pls1 is a tetraspanin-like protein required for penetration of the leaf cuticle and has a similar phenotype to the *Δnox2* mutant in *M. oryzae, P. anserina* and *B. cinerea* (Clergeot et al., 2001; Lambou et al., 2008; Siegmund et al., 2013). It has also been suggested that *PLS1* is associated with *NOX2* activity as they have similar mutant phenotypes, both with disorganised F-actin, septin and Chm1 rings (Ryder et al., 2013; Tudzynski et al., 2012). It has been proposed that Pls1 may be involved in the recruitment of Nox2 to the plasma membrane, playing a similar role to p22phox orthologue NoxD, which is believed to be involved in the recruitment of Nox1 to the plasma membrane in both *P. anserine* and *B. cinerea* (Lacaze et al., 2015; Siegmund et al., 2015).

1.4 Introduction to the current study

I set out to understand the organisation of the components of the Nox signalling complex in *M. oryzae*. To do this I utilised the yeast two-hybrid method to study the physical protein-protein interactions of putative Nox associated proteins. I also carried out gene functional analysis by targeted gene replacement. The

results of these investigations are presented and discussed in the context of understanding the biology of plant infection in *M. oryzae*.

2. Methods and Materials

2.1 Maintenance and growth of *M. oryzae* strains

All strains of *M. oryzae* used during the study were grown on complete medium (CM) and incubated at 25°C with a 12 hour light/dark photoperiod. CM contains: 10 g/L glucose, 2 g/L peptone, 1 g/L yeast extract (BD Biosciences), 1 g/L casamino acids, 0.1 % (v/v) trace elements (22 mg/L zinc sulphate heptahydrate, 11 mg/L boric acid, 5 mg/L manganese (II) chloride tetrahydrate, 1.6 mg/L cobalt (II) chloride hexahydrate,1.6 mg/L copper (II) sulphate pentahydrate, 1.5 mg/L sodium molybdate dehydrate, 50 mg/L ethylenediaminetetraacetic acid), 0.1 % (v/v) vitamin solution (0.1 µg/L biotin, 0.1 µg/L pyridoxin, 0.1 µg/L thiamine, 0.1 µg/L riboflavin, 0.1 µg/L p-aminobenzoic acid, 0.1 µg/L nicotinic acid), Nitrate salts (6 g/L sodium nitrate, 0.5 g/L potassium chloride, 0.5 g/L magnesium sulfate heptahydrate, 1.5 g/L potassium dihydrogen phosphate), 15 g/L agar adjusted to a pH to 6.5 with 1M sodium hydroxide. Liquid cultures were made using CM excluding the agar. All chemicals were supplied from sigma unless otherwise specified. Long term storage of *M. oryzae* strains were grown over filter discs (3mm, Whatmann International) and desiccated for 3 days at room temperature and stored at -20°C onwards.

2.2 *M. oryzae* nucleic acid extraction

2.2.1 Fungal genomic DNA extraction

A plug of *M. oryzae* was inoculated onto a cling film disc (Lakeland) on a CM agar plate. Cultures were incubated for 8 days at 24°C or until a lawn of mycelium covered the cellophane discs. Cellophane discs were peeled off and ground to a

fine powder in a mortar with liquid nitrogen. Powder was then decanted into 2 ml microfuge tubes before being stored at -80°C. An aliquot of 500 µl 2 X CTAB buffer (20 g/L CTAB, 12 g/L Tris, 2.92 g/L EDTA and 41 g/L sodium chloride), preheated to 65 ºC was added and incubated at 65°C for 30 minutes with occasional shaking every 10 minutes. An equal volume of chloroform:isopropanol alcohol (24:1) was added and incubated for 20 minutes with 400 rpm on a shaking platform (IKA®) at room temperature. Samples were centrifuged for 20 minutes at 16000 *x g* and the top phase supernatant was removed into eppendorfs. The step was repeated and the final supernatant was transferred to a clean 1.5 ml eppendorf. To precipitate the nucleic acids 1 ml of chilled Isopropanol was added mixed and incubated overnight at -20°C. The DNA was pelleted by centrifugation at 16000 *x g* for 10 minutes at 4°C. The supernatant was removed and allowed to drain, the remaining pellet was re-suspended in 500 µl nuclease-free-water. The DNA was re-precipitated using 50 µl of 3 M sodium acetate (pH 5.3) and 1 ml of chilled absolute ethanol and incubated for 10 minutes at -20 °C. The DNA was recovered by centrifugation at 16000 *x g* for 20 minutes at room temperature. The pelleted DNA was washed with 70% (v/v) ethanol and centrifuged for 5 minutes at 16000 *x g*. The supernatant was discarded and dried in a speed vac for 10 minutes before the pellet was re-suspended in 50 µl nuclease-free-water and 2 µl RNase A (10 µg/ml). Samples were stored at -20°C and analysed using a NanoDrop Spectrophotometer (Thermo Scientific).

2.2.2 Conidial RNA extraction

Conidia were harvested from 10-day old *M. oryzae* Guy 11 plates (as described later in section 2.9.1.) into a 2 ml eppendorf. Conidia were pelleted using centrifugation at 9600 *x g* for 5 minutes and the supernatant was removed. A metal bead was added to the tube and placed in liquid nitrogen cooled tissue

lyser (Qiagen, Tissue Lyser II) and shaken for 1 minute at a frequency of 18 Hz. RNA extraction was performed using the material produced and the commercial kit, RNeasy® Plant Mini Kit from Qiagen, according to the manufacturer's instructions. To disrupt the sample further, 400 µl of buffer RLT was added, vortexed. The lysate was transferred to a QIAshredder spin column for centrifugation at top speed for 2 minutes. The supernatant was recovered and 0.5 volume of ethanol was added and immediately transferred to an RNeasy Mini spin column for centrifugation at 8,000 *x g* for 15 seconds. The column was washed with 700µl of buffer RW1 followed by 500 µl buffer RPE by centrifugation at 8,000 *x g* for 15 seconds. A final wash with 500 µl of buffer RPE at 8,000 *x g* for 2 minutes. The total RNA was eluted from the column with 50 µl of RNase-free water. The samples were stored at -80°C and analysed using a Nanodrop Spectrophotometer (Thermo Scientific).

2.3 DNA manipulations

2.3.1 Digestion of genomic or plasmid DNA with restriction endonucleases

Digestion using restriction endonucleases were used for confirmation of fungal transformants via Southern blot analysis as well as digestion to produce linearized plasmid DNA. All restriction endonucleases used were supplied by New England Biolabs Inc. Typically 0.1-0.5 µg of DNA was digested in a total volume of 30 µl using 5-10 units of enzyme and incubated at 37°C overnight. For Southern blot analysis 15 µg of DNA was digested in a total volume of 30 µl with 20 units of enzyme and incubated at 37°C overnight. All digestions were carried out using the appropriate buffer supplied by the manufacturers.

2.3.2 Gel Electrophoresis

All DNA analysis through gel electrophoresis was carried out in 0.8% (w/v) agarose gel with 1x TBE buffer (90 mM Tris-borate, 2 mM EDTA) with 4 µg of

ethidium bromide (10 mg/ml) per 100 ml 1x TBE buffer. The use of ethidium bromide allowed visualisation of fragments via a UV transilluminator (UVP BioDoc-It®). To determine the DNA fragment length a 1kb plus DNA ladder (Invitrogen) was used.

2.3.3 Gel purification

Gel purification was carried out using Wizard® SV Gel and PCR Clean Up System kit (Promega, UK) according to the manufacturer's instructions. Fragments were excised using a razor blade and the mass of the gel slice was determined. An equal volume of Membrane Binding Solution (4.5 M guanidine isothiocyanate, 0.5 M potassium acetate (pH 5)) was added and incubated at 65°C to dissolve the gel slice. The gel mixture was then transferred to the Wizard® SV Minicolumn assembly and incubated for one minute before centrifugation at 16,000 *x g* for 1 minute. The column was washed using 700 µl Membrane Wash Solution (10 mM potassium acetate (pH 5), 80% ethanol, 16.7 mM EDTA (pH 8)) and centrifuged at 16,000 *x g* for 1 minute. The step was repeated with 500 µl Membrane Wash solution and centrifuged at 16,000 *x g* for 5 minutes. After the washes the column was further centrifuged at 16,000 *x g* for 1 minute to remove residual ethanol. To elute the final DNA the Wizard® SV Minicolumn was transferred to a sterile eppendorf and 50 µl of nuclease-free water was added and incubated for 1 minute before centrifugation at 16,000 *x g* for 1 minute. The eluted DNA was analysed using a NanoDrop (Thermo Scientific) and stored at -20°C.

2.3.4 Amplification of DNA by Polymerase Chain Reaction (PCR)

Amplification of target DNA was performed using an Applied Biosystems® Veriti™ 96 Well Thermal Cycler. DNA polymerases used included GoTaq® Green Master Mix (Promega, UK), Phusion® High Fidelity (NEB), SapphireAmp® Fast

PCR Master Mix (Takara Bio Inc.) and In-Fusion® (Takara Bio Inc.). All primers were synthesised by Eurofins Genomics. A typical reaction using GoTaq® Green Master Mix included: Gotaq® Green Master Mix (2x), 50 ng template DNA, 10 µM of each primer and nuclease-free water to a final volume of 30 µl. Amplification conditions were: Initial denaturation at 95 °C for 5 minutes followed by 35 cycles of 95°C for 30 seconds, 57-65 °C for 30 seconds, 72 °C for 1 minute/kb and a final extension of 72 °C for 5 minutes. A typical reaction using Phusion® included: 1 unit of Phusion DNA polymerase, 100 ng template DNA, 10 µM of each primer, 5X GC or HF buffer, 10 mM dNTPs and nuclease free water to a final volume of 25 µl. Amplification conditions were: Initial Denaturation at 98 °C for 10 seconds, 35 cycles of 98 °C for 10 seconds, 57-65 °C for 30 seconds and 72 °C for 30 seconds/kb and a final extension at 72 °C for 10 minutes.

2.3.5 cDNA synthesis – reverse transcription PCR

Synthesis of cDNA from *M. oryzae* RNA was performed using the AffinityScript QPCR cDNA Synthesis Kit (Agilent Technologies). For a 20 µl reaction, this included: cDNA Synthesis Master Mix (2X), AffinityScript RNase Block Enzyme Mixture, 100 mg/µl Oligo(dT) primer, 1 µg template RNA and nuclease-free water to a final volume of 20 µl. The Amplification conditions were: 25 °C for 3 minutes, 42 °C for 15 minutes and to terminate cDNA synthesis 95 °C for 5 minutes.

2.4 DNA cloning procedures

2.4.1 DNA ligation

PCR amplified fragments were ligated into linearized pGADT7 and pGBKT7 vectors (Clontech Inc.) (**Figure 2.1a**) using the In-fusion® HD Cloning Kit (Takara Bio Inc.). A typical reaction of using In-Fusion®: 5X In-Fusion HD Enzyme

Premix, 50 ng linearized vector, 50 ng purified cDNA, and nuclease-free water to a total volume of 10 µl. Ligation conditions were: 15 minutes at 50 °C.

2.4.2 Bacterial vector transformation and positive recombinant clonal selection

Plasmids produced by ligation were transformed into competent Stellar™ *Escherichia coli* strain HST08 (Takara Bio Inc). To a polypropylene tube 2.5 µl of the final ligation and 50 µl of competent cells were added and incubated on ice for 30 minutes. The mixture was heat shocked at 42 °C for 45 seconds and returned to ice. After 2 minutes 500 µl of SOC medium (2% (v/v) tryptone, 0.5% (v/v) yeast extract, 10mM sodium chloride, 2.5 mM potassium chloride, 20 mM glucose, 10 mM magnesium sulfate, 10 mM magnesium chloride) preheated to 37 °C was added and incubated with shaking at 37 °C for an hour. From the final volume 100 µl was spread on LB medium (10 g/L tryptone, 5 g/L yeast extract, 5 g/L sodium chloride (pH 7.5), 18 g/L agar) with the correct selective antibiotic and incubated at 37 °C overnight (**Table 2.1**).

Vector	Bacterial selection marker	Yeast selection marker
pGBKT7	Kanamycin	Tryptophan
pGADT7	Ampicillin	Leucine
pGBKT7-53	Kanamycin	Tryptophan
pGADT7-T	Ampicillin	Leucine

Table 2.1 Yeastmaker™ Plasmid Selection Information.

Confirmation of recombinant clones was determined using colony PCR. A typical reaction using SapphireAmp®: SapphireAmp® Fast PCR Master Mix (2X Premix), a sample of a selected colony as template DNA, 10 µM of each primer (**Table 2.2**) and nuclease-free water to a final volume of 50 µl. Amplification

conditions were: Initial denaturation at 98 °C for 2 minutes, 35 cycles of 98 °C for 5 seconds, 58 °C for 5 seconds and 72 °C for 10 seconds/kb and a final extension of 72 °C for 7 minutes. To check for positive recombinant clones, each reaction was analysed using gel electrophoresis as described in section 2.3.2.

Table 2.2 Primers used for amplification of cDNA inserts.

Gene	Gene ID (MGG_)	Primer name	Primer Sequence
NOX1	00750	Nox1_ pGADT7F	GGAGGCCAGTGAATTCATGTCGGT CGGAGAGTTCTTGGCT
		Nox1_ pGADT7R	CGAGCTCGATGGATCCCTAGAAAT GCTCCTTCCAGAAGCG
NOX2	06559	Nox2_ pGBKT7F	CATGGAGGCCGAATTCATGTCTGG ATACGGCTACGGAGGA
		Nox2_ pGBKT7R	GCAGGTCGACGGATCCCTAGAAAT TCTCCTTGCCCCATAC
		Nox2_ pGADT7F	GGAGGCCAGTGAATTCATGTCTGG ATACGGCTACGGAGGA
		Nox2_ pGADT7R	CGAGCTCGATGGATCCCTAGAAATT CTCCTTGCCCCATAC
NOX3	08299	Nox3_ pGBKT7F	CATGGAGGCCGAATTCATGGCCAA GAGCACAACTACCGAT
		Nox3_ pGBKT7R	GCAGGTCGACGGATCCCTAGTTGA AAACCTCAATCATAAA
RAC1	02731	Rac1_ pGBKT7F	CATGGAGGCCGAATTCATGGCCGC CCCTGGGGTTCAGTCT
		Rac1_ pGBKT7R	GCAGGTCGACGGATCCTCACAGAA TGGTGCACTTTGACTT
PLS1	12594	Pls1_ pGBKT7F	CATGGAGGCCGAATTCATGGCGAA CAAGATTCTCGTGGCG
		Pls1_ pGBKT7R	GCAGGTCGACGGATCCTCACAGAG TGCTCATCGGGCCGGT
		Pls1_ pGADT7F	GGAGGCCAGTGAATTCATGGCGAA CAAGATTCTCGTGGCG
		Pls1_ pGADT7R	CGAGCTCGATGGATCCTCACAGAG TGCTCATCGGGCCGGT
CHM1	06320	Chm1_ pGBKT7F	CATGGAGGCCGAATTCATGGCGTC GCAAAACAACATGTAT

		Chm1_pGBKT7R	GCAGGTCGACGGATCCTTATTTGG CATGCTTCTTGAAGGC
		Chm1_ pGADT7F	GGAGGCCAGTGAATTCATGGCGTC GCAAAACAACATGTAT
		Chm1_pGADT7R	CGAGCTCGATGGATCCTTATTTGGC ATGCTTCTTGAAGGC
CDC24	09697	Cdc24_pGBKT7F	CATGGAGGCCGAATTCATGGCATAT GCGCCCCTCTTGAGA
		Cdc24_pGBKT7R	GCAGGTCGACGGATCCCTACTCGC CACCAATGCCAACGCA
		Cdc24_pGADT7F	GGAGGCCAGTGAATTCATGGCATA TGCGCCCCTCTTGAGA
		Cdc24_pGADT7R	CGAGCTCGATGGATCCCTACTCGC CACCAATGCCAACGCA
CDC42	00466	Cdc42_pGBKT7F	CATGGAGGCCGAATTCATGGTGGT TGCAACGATTAAATGC
		Cdc42_pGBKT7R	GCAGGTCGACGGATCCTCAAAGGA TCAGGCACTTTTTGGA
		Cdc42_pGADT7F	GGAGGCCAGTGAATTCATGGTGGT TGCAACGATTAAATGC
		Cdc42_pGADT7R	CGAGCTCGATGGATCCTCAAAGGA TCAGGCACTTTTTGGA
BEM1	01702	Bem1_pGBKT7F	CATGGAGGCCGAATTCATGAAGGC CTTACGGCGATCCATC
		Bem1_pGBKT7R	GCAGGTCGACGGATCCTTATATGT GATCAACGTAGAACAA
		Bem1_pGADT7F	GGAGGCCAGTGAATTCATGAAGGC CTTACGGCGATCCATC
		Bem1_pGADT7R	CGAGCTCGATGGATCCTTATATGTG ATCAACGTAGAACAA
MAS1	04202	Mas1_pGBKT7F	CATGGAGGCCGAATTCATGAAGTA CACCAGCGCCATCCTC
		Mas1_pGBKT7R	GCAGGTCGACGGATCCCTACTCGT CATCCTCCTCGTCGGT

2.4.3 Bacterial plasmid extraction

A positive single colony was picked from an agar plate, re-suspended in 50 ml of LB medium and incubated with 125 rpm shaking overnight at 37 °C. For purification of bacterial plasmid DNA of bacteria the PureYield™ Plasmid Midiprep System (Promega, Corporation) and used according to the manufacturer's instructions. Bacterial cultures were centrifuged at 5,000 *x g* for 10 minutes at 4 °C and the pellet was re-suspended in 3 ml of Cell Resuspension Solution (50 mM Tris-HCL (pH 7.5), 10 mM EDTA (pH 8), 100 µg/ml RNase). A 3 ml aliquot of Cell Lysis Solution (0.2 M sodium hydroxide, 1% sodium dodecyl sulfate) was added and mixed by inversion. After a 3 minute incubation at room temperature 5 ml of Cell Neutralisation Solution (4.09 guanidine hydrochloride (pH 4.2), 0.759 M potassium acetate, 2.12 M glacial acetic acid) was added and mixed by inversion. The sample was centrifuged at 15,000 *x g* at 4 °C for 15 minutes. DNA purification was eluted using a vacuum manifold (ILMVAC) using the PureYield™ Clearing Column placed on top of the PureYield™ Binding Column. The supernatant was poured into the column assembly and the vacuum was applied. The PureYield™ Clearing column was discarded and 5 ml of Endotoxin Removal Wash (0.2 M sodium hydroxide, 1% sodium dodecyl sulfate) was added to the clearing column with the vacuum applied. Once the liquid had been pulled through, 20 ml of Column Wash (162.8 mM potassium acetate, 22.6 mM Tris-HCL (pH7.5), 0.109 mM EDTA (pH 8)) was added and after the solution was pulled through the column was allowed to dry. To elute the purified plasmid DNA, 600 µl of nuclease-free water was added to the PureYield™ Binding Column which was placed into a falcon tube and the assembly was centrifuged at 1,500 rpm for 5 minutes. Each plasmid construct was sequenced by Eurofins

to confirm the correct sequence and alignment. Plasmid DNA was routinely stored at -4°C.

2.5 Yeast Transformation

Transformation of yeast was performed using Yeastmaker™ Yeast Transformation System 2 kit (Clontech Laboratories, Inc.) according to the manufacturer's instructions. One colony of the *Saccharomyces cerevisiae* Y2HGold strain was picked out from a YPDA plate (20 g/L peptone, 10 g/L yeast extract, 20g/L dextrose, 20 g/L agar, 40 mg/L adenine hemisulfate) and incubated in 15 ml of YPD liquid medium (20 g/L peptone, 10 g/L yeast extract, 20 g/L dextrose) overnight at 30 °C with 220 rpm shaking. The culture was transferred to a flask of 300 ml YPD liquid medium and incubated for 3 hours at 30 °C with 220 rpm shaking. This was centrifuged at 700 *x g* for 5 minutes and the resulting pellet was re-suspended in 15 ml of sterile, deionised water and centrifuged again using the same conditions. The pellet was re-suspended in 1.5 ml 1.1 x TE/LiAc, pH 7.5 (diluted from a 10 x stock: 1 M lithium acetate, TE buffer (0.1 M Tris-HCL, 10 mM EDTA)) and transferred into a microcentrifuge tube for high speed centrifugation for 15 seconds. The supernatant was discarded and the pellet re-suspended in 600 µl 1.1 x TE/LiAc. To transform 50 µl of the purified cells, 200 ng of each plasmid DNA seen in **Figure 2.1b**, 50 µl of denatured herring sperm (10mg/ml, 0.1 M sodium chloride) and 500 µl of PEG/LiAc (40% polyethylene glycol 4000, 1 X TE buffer, 1 X lithium acetate) were incubated in a microcentrifuge tube at 30 °C for 30 minutes with occasional inversion. The mixture was transferred to a 42 °C heat block (Stuart SBHI 30D Block Heater) for 15 minutes with occasional inversion. The cells were pelleted using high speed centrifugation for 15 seconds and re-suspended in 200 µl of sterile, deionised

water. The culture was plated out in 200 µl aliquots on appropriate selective medium. This was repeated for each plasmid found in **Figure 2.1b**.

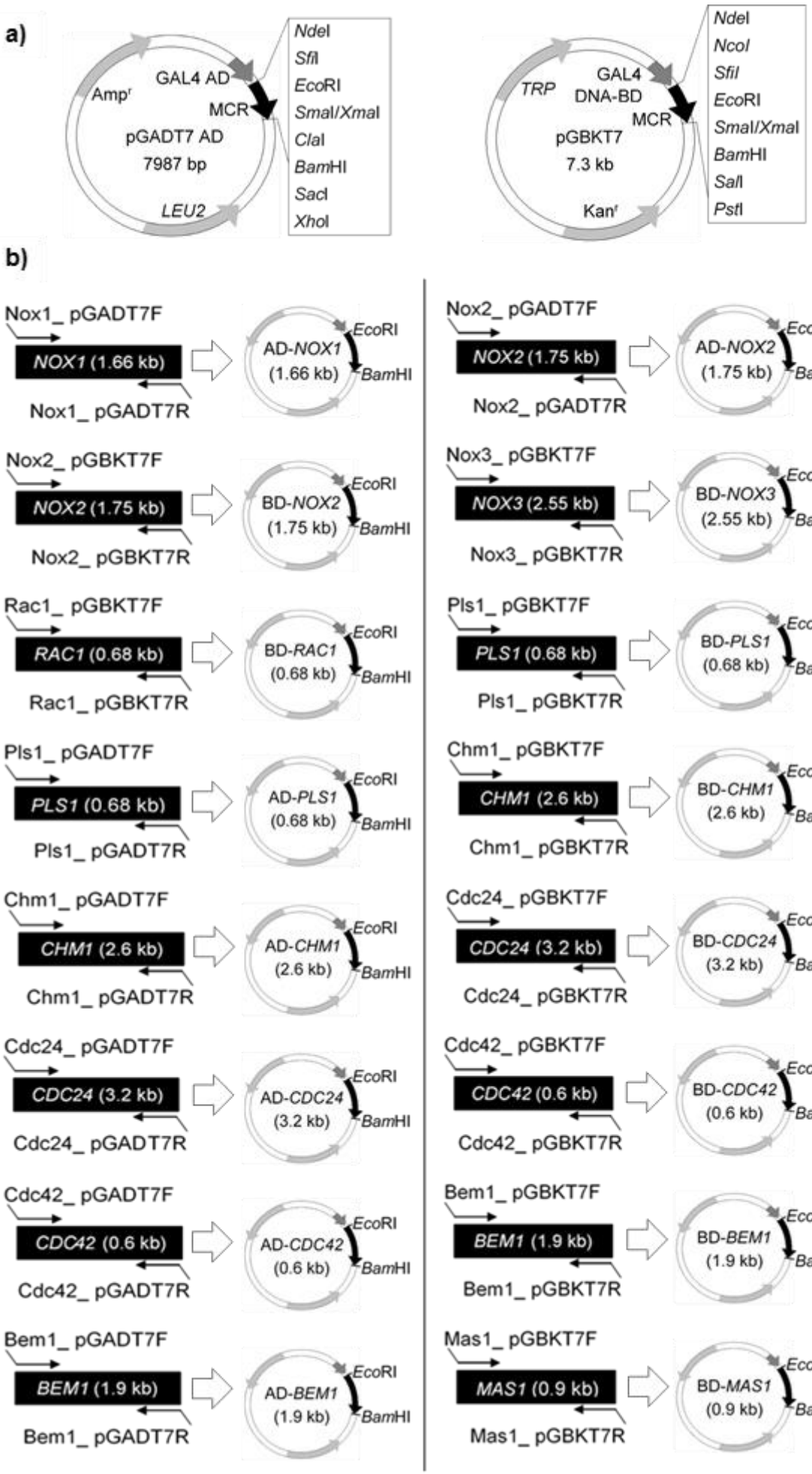
a)
GAL4 AD
Amp^r
MCR
pGADT7 AD
7987 bp
LEU2
NdeI
SfiI
EcoRI
SmaI/XmaI
ClaI
BamHI
SacI
XhoI
TRP
GAL4
DNA-BD
MCR
pGBKT7
7.3 kb
Kan^r
NdeI
NcoI
SfiI
EcoRI
SmaI/XmaI
BamHI
SalI
PstI
b)
Nox1_ pGADT7F
NOX1 (1.66 kb)
Nox1_ pGADT7R
AD-NOX1
(1.66 kb)
Nox2_ pGBKT7F
NOX2 (1.75 kb)
Nox2_ pGBKT7R
BD-NOX2
(1.75 kb)
Rac1_ pGBKT7F
RAC1 (0.68 kb)
Rac1_ pGBKT7R
BD-RAC1
(0.68 kb)
Pls1_ pGADT7F
PLS1 (0.68 kb)
Pls1_ pGADT7R
AD-PLS1
(0.68 kb)
Chm1_ pGADT7F
CHM1 (2.6 kb)
Chm1_ pGADT7R
AD-CHM1
(2.6 kb)
Cdc24_ pGADT7F
CDC24 (3.2 kb)
Cdc24_ pGADT7R
AD-CDC24
(3.2 kb)
Cdc42_ pGADT7F
CDC42 (0.6 kb)
Cdc42_ pGADT7R
AD-CDC42
(0.6 kb)
Bem1_ pGADT7F
BEM1 (1.9 kb)
Bem1_ pGADT7R
AD-BEM1
(1.9 kb)
Nox2_ pGADT7F
NOX2 (1.75 kb)
Nox2_ pGADT7R
AD-NOX2
(1.75 kb)
Nox3_ pGBKT7F
NOX3 (2.55 kb)
Nox3_ pGBKT7R
BD-NOX3
(2.55 kb)
Pls1_ pGBKT7F
PLS1 (0.68 kb)
Pls1_ pGBKT7R
BD-PLS1
(0.68 kb)
Chm1_ pGBKT7F
CHM1 (2.6 kb)
Chm1_ pGBKT7R
BD-CHM1
(2.6 kb)
Cdc24_ pGBKT7F
CDC24 (3.2 kb)
Cdc24_ pGBKT7R
BD-CDC24
(3.2 kb)
Cdc42_ pGBKT7F
CDC42 (0.6 kb)
Cdc42_ pGBKT7R
BD-CDC42
(0.6 kb)
Bem1_ pGBKT7F
BEM1 (1.9 kb)
Bem1_ pGBKT7R
BD-BEM1
(1.9 kb)
Mas1_ pGBKT7F
MAS1 (0.9 kb)
Mas1_ pGBKT7R
BD-MAS1
(0.9 kb)
EcoRI
BamHI

Figure 2.1 Schematic for each PCR fragment ligated into the correct vector for yeast two-hybrid.

a) The pGADT7 and pGBKT7 vector maps with multiple cloning region and restriction digest sites indicated. **b)** Each putative protein partner was amplified from cDNA and ligated into the appropriate vector to form the recombinant plasmid.

2.6 Screening yeast transformations

Yeast cells were plated on minimal SD dropout medium (1.71 g/L yeast nitrogen base without amino acid and ammonium sulfate, 5 g/L ammonium sulfate, 20 g/L glucose, 20 g/L agar) with dropout supplement (200 mg/L L-adenine hemisulfate salt, 200 mg/L L-Arginine HCL, 200 mg/L L-histidine HCL monohydrate, 300 mg/L L-Isoleucine, 1000 mg/L L-Leucine, 300 mg/L L-lysine HCL, 200 mg/L L-Methionine, 500 mg/L L-Phenylalanine, 2000 mg/L L-Threonine, 200 mg/L L-Tryptophan, 300 mg/L L-Tyrosine, 200 mg/L L-Uracil, 1500 mg/L L-Valine). Nutrients were excluded to select for transformants containing the ligated plasmids (**Table 2.1**). For *MEL1* reporter expression assays, 20 mg/ml of x-α-gal (Melford Laboratories) in dimethylformamide was added to the dropout medium. Plates were inverted and incubated at 30 °C for 5-7 days.

2.7 DNA-mediated *M. oryzae* transformation

A 2.5 cm² section of *M. oryzae* mycelium was excised from an agar plate culture, blended in 150 ml of liquid complete medium and 150 µl of penicillin/streptomycin Stock (50 mg/ml of each) and incubated at 25 °C with shaking at 125 rpm for 48 hours. The mycelium were harvested via filtration through a sterile miracloth (Calbiochem) and washed using sterile deionised water. The mycelium were dried and transferred to a 50 ml falcon tube (Greiner Bio-One) with 40 ml of filter sterilised OM buffer (1.2 M magnesium sulfate heptahydrate, 10 mM sodium

phosphate (pH 5.8), 5% Glucanex (Novozymes)) adjusted to pH 5.6 and incubated at 30 °C for 3 hours with 75 rpm shaking. The resulting mixture was transferred to sterile polycarbonate Oakridge tubes (Nalgene^{TM}) and overlaid with cold autoclaved ST buffer (0.6 M Sorbitol, 0.1 M Tris-HCL (pH 7)). The Oakridge tubes were centrifuged using a swinging bucket rotor (Beckman J2 MC) at 5,000 *x g* for 15 minutes at 4 °C. The protoplasts were recovered from the OM/ST interface, re-suspended in cold autoclaved STC buffer (1.2 M sorbitol, 10 mM Tris-HCL (pH 7.5), 10 mM calcium chloride) and centrifuged at 3000 *x g* at 4°C for 10 minutes. The resulting pellet was washed with 10 ml of STC buffer and centrifuged again with the same conditions. This step was repeated with complete re-suspension each time and the final pellet was re-suspended in 1 ml of STC buffer. The concentration of protoplasts was determined using a haemocytometer and diluted to a concentration of 5 x 10^6 / ml. In a 1.5 ml eppendorf 4 µg of DNA of the two hygromycin cassette amplicons, produced used the primers in **Table 2.3,** were combined with protoplasts in a final volume of 150 µl and incubated at room temperature for 20 minutes. After incubation 1 ml of PTC buffer (60% (w/v) polyethylene glycol, 10 mM Tris-HCL (pH 7.5) and 10 mM calcium chloride) was added, inverted and incubated at room temperature for 20 minutes. The protoplast mixture was added and mixed by gentle inversion into 150 ml of molten OCM (osmotically controlled medium: complete medium, 0.8 M sucrose) and poured into 5 plates. The plates were incubated in the dark at 24 °C for 18 hours for selection under hygromycin B, plates were overlaid with complete medium containing 300 µg/ml hygromycin B (Millipore corp).

Table 2.3 Primers used for split marker deletion of *PLS1.*

Primer name	Sequence (5'→3')
50.1_PLS1F	GCCATGGAATCCTCTCCTTCATTG
50.1_PLS1R	GTCGTGACTGGGAAAACCCTGGCGCGCCATCGTGAAAAA GTGAGAGGT
30.1_PLS1F	TCCTGTGTGAAATTGTTATCCGCTAGCACTCTGTGAGCGT CTTGAATC
30.1PLS1R	CAGGCGGCTAAATAATTGGATACC
M13F	CGCCAGGGTTTTCCCAGTCACGAC
M13R	AGCGGATAACAATTTCACACAGGA
HY split	GGATGCCTCCGCTCGAAGTA
YG split	CGTTGCAAGACCTGCCTGAA

Flanking reverse complement M13F and M13R sequence is shown underlined.

2.8 Southern blot analysis

Southern blot analysis was performed according to the method of Sambrook et al., 1989. Extracted genomic DNA was digested using appropriate restriction endonucleases overnight to allow complete digestion. The digested DNA was run overnight in a 0.8% TBE agarose gel at 16 V to allow separation by size. The gel was soaked in 0.25 M HCl for 15 minutes in order to de-purinate the fractioned DNA and then denatured by immersing in southern denaturing solution (0.4 M sodium hydroxide, 0.6 M sodium chloride) for 30 minutes with gentle rocking. The gel was transferred to neutralisation solution (1.5 M sodium chloride, 0.5 M Tris-HCL (pH 7.6)) for 30 minutes with gentle rocking before capillary blotting onto Hybond-N nylon membrane (Amersham Biosciences). Gel blots were performed by placing the inverted gel onto a sheet of filter paper wick, which was supported on a perspex sheet with each end of the wick submerged in 20 x SSPE solution (3.6 M sodium chloride, 0.2 M sodium dihydrogen phosphate, 22 mM EDTA). Hybond-N nylon membrane was then placed onto the gel and overlaid with five layers of wet 3 mm Whatmann paper soaked in 20X SSPE, five layers of dry 3

mm Whatmann paper and a stack of towels (Kimberly Clark Corporation). Finally, a weight was applied on top of the stack and the blot was left at room temperature overnight. The assembly was dismantled after blotting overnight and the membrane dried before UV-crosslinking (Uvitec) to fix the DNA to the membrane.

2.8.1 Radio-labelled probe production

For confirmation of positive fungal transfomants a radio-labelled probe was produced using Prime-It RmT Random Primer Labeling Kit (Agilent Technologies) according to the manufacturer's instructions. The supplied single use reaction tubes (random primers, dNTPs, Buffer and cofactors) were rehydrated with 46 µl of nuclease-free water and 100 ng of probe DNA. The sample was denatured at 100 °C for 5 minutes and placed on ice for 2 minutes. The tube was briefly centrifuged and 2 µl of magenta DNA polymerase and 1-2 µl of [α-^{32}P] dCTP (3000Ci/mmol) were added and incubated at 37 °C for 10 minutes on a block heater (Stuart Equipment). The reaction was stopped with 100 µl of labelling stop dye (0.1% sodium dodecyl sulfate, 60 mM EDTA, 0.5% Bromophenol Blue, 1.5% Blue Dextran). The reaction was added to a Biogel column containing glass wool and Biogel P60 (BioRad) and kept hydrated using 20 X TELS (200 mM Tris, 2 mM disodium EDTA, 4% sodium dodecyl sulfate). The light blue fraction of labelled probe was collected and boiled at 100 °C for 5 minutes and then cooled on ice for 2 minutes before adding to the hybridisation mixture.

2.8.2 Hybridisation

UV fixed blots were incubated in hybridisation bottles (Hybaid) containing 30 ml of Pre-hybridisation solution (6 X SSPE (diluted from 20 X SSPE: 3.6 M sodium chloride, 0.2 M sodium dihydrogen phosphate, 22 mM EDTA), 5 X Denhardt's (diluted from 100 X Denhardts: 2 % Polyvinlypyrrolidone 360,000, 2 % Ficoll

400,000, 32 % bovine serum albumen), 0.5 % sodium dodecyl sulfate) and 1 ml of denatured herring sperm (10mg/ml, 0.1 M sodium chloride) at 65 °C for 4 hours in an incubator oven (Hybaid). The radio-labelled probe was added and returned to the incubator for 18 hours incubation. The solution was discarded and the membrane washed for 30 minutes with 2 X SSPE (2 X SSPE (diluted from 20 X SSPE: 3.6 M sodium chloride, 0.2 M sodium dihydrogen phosphate, 22 mM EDTA), 0.1% sodium dodecyl sulfate, 0.1% sodium pyrophosphate) and then replaced with 0.2 % SSPE wash solution (0.2 X SSPE (diluted from 20 X SSPE: 3.6 M sodium chloride, 0.2 M sodium dihydrogen phosphate, 22 mM EDTA), 0.1 % sodium dodecyl sulfate, 0.1% sodium pyrophosphate) for a further 30 minutes at 65 °C. The membrane was then removed from the bottle and dried DNA side up before it was wrapped in cling film and placed in a photographic cassette with X-ray film (Fuji medical X-ray film) for visualisation of the hybridisation. The cassette was stored at -80 °C and were developed using an Opitmax film processor (Protec).

2.9 Pathogenicity and infection-related development assays

2.9.1 Rice blast infection assays

Infection assays were carried out using a dwarf Indica rice (*Oryza sativa*) cultivar, CO-39 which is susceptible to *M. oryzae* (Valent & Chumley, 1991). *M. oryzae* cultures were grown for 10 days on CM plates and conidia were harvested using 5 ml of sterile de-ionised water. The suspension was filtered through miracloth (Calbiochem) and centrifuged (VWR, Micro Star 17) at 9600 *x g* for 5 minutes. The remaining pellet was re-suspended in 0.2% gelatine to a final concentration of $1x10^4$ conidia ml^{-1}. Rice was grown in 9 cm diameter pots with 7 plants per pot. Three pots of 14-day-old plants were used per strain when spraying with the prepared inoculum using an artist's airbrush (Badger Airbrush, Franklin Park,

Illinois, USA) to disperse the suspension. After spraying, the plants were covered with a plastic bag for 48 hours after which the bag was removed. The plants were grown for 5 days post inoculation in a controlled environment growth room at 24°C with a 12 hour light/dark cycle at 90% relative humidity before the leaves were harvested to record lesion density.

2.9.2 Leaf sheath infection assay

Using a razor blade, sections of 14-day-old CO-39 were excised from the rice plant and placed flat in a square petri dish (Greiner Bio-One). Conidia were harvested (as described in section 2.9.1) and re-suspended to a final concentration of $1x10^5$ conidia per ml in 0.2% gelatine. An aliquot of 50 µl of the spore suspension was placed onto the leaf sheath, on the same leaf a Guy11 spore suspension was added to act as a control. The inoculated samples were incubated in a controlled environment chamber at 24 °C with a 12 hour light/dark cycle with high humidity for 4-5 days post inoculation.

3. Results

3.1 Identifying components of the Nox1 and Nox2 multi-protein complex in *M. oryzae* using the yeast two-hybrid system

The proteins included in the study are putative interactors of the Nox complex or Nox complex components. Nox flavoenzymes investigated in the study are Nox1, Nox2 and Nox3. Pls1 is a tetraspanin like protein and has been proposed to have an association with Nox2 because *ΔPLS1* mutants of *M. oryzae, P. anserina* and *B. cinerea* have similar phenotypes to mutants lacking *NOX2* (Gourgues et al., 2004; Lambou et al., 2008; Ryder et al., 2013). Evidence by yeast two-hybrid assays have also found interactions between the mammalian $p67^{phox}$ homologue, NoxR and yeast polarity proteins Cdc24 and Bem1 (Takemoto et al., 2011). Other

putative components include the Rho-family GTPases Cdc42 and Rac1. Rac1 interacts with Nox1, Nox2 and the PAK kinase Chm1 in yeast two-hybrid assays and is activated by the guanine nucleotide exchange factor (GEF) Cdc24 (Chen et al., 2008; Takemoto et al., 2011). Mas1 is a gene specifically expressed in appressoria in *M. oryzae* (Xue et al., 2002). PKC is a protein kinase and has evidence to suggest involvement in Nox regulation via phosphorylation (Sumimoto et al., 2005).

The Yeast Two-Hybrid assays were performed using the YeastmakerTM Yeast Transformation System 2 kit (Clontech Laboratories, Inc.). This system is under the control of 3 Gal4-responsive promoters with 4 reporter genes: AUR1-C, HIS3, ADE2 and MEL1. To identify protein partners of the Nox complex, proteins are expressed fused to the Gal4 DNA-binding-domain (DNA-BD) and a putative partner, to a Gal4 activation domain (AD). The DNA-BD and AD are expressed on pGBKT7 and pGADT7 vectors respectively. These vectors contain bacterial selection markers to allow isolation and extraction of the plasmid. The vectors also contain yeast selection markers to allow selection of positive transformed cells on selection medium. A positive control is performed using control vectors (pGBKT7-53 and pGADT7-T) which are known to interact and negative control was accomplished using empty vectors (pGBKT7 and pGADT7). When there is a positive interaction between two proteins it brings the two domains within proximity and activates transcription of the four reporter genes (**Figure 3.1**).

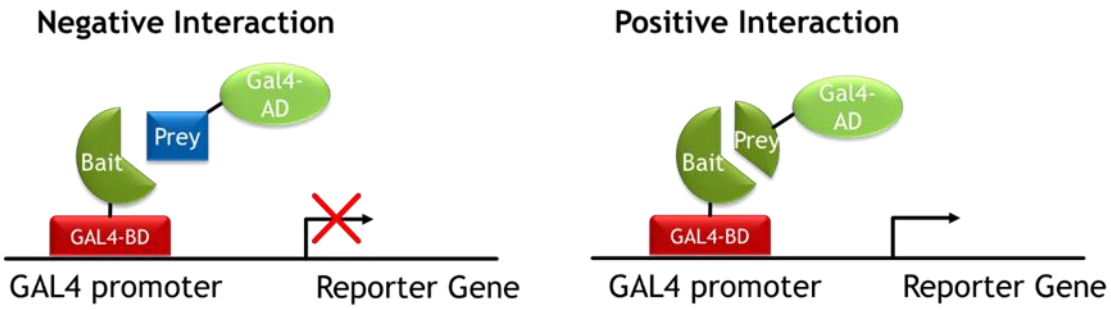

Figure 3.1 The theory of Yeast Two-Hybrid.

Two proteins are expressed, one fused to the Gal4 DNA-activation domain (AD) and the other to the Gal4 DNA-Binding domain (BD). The four independent reporter genes (*AUR1-C*, *ADE2*, *HIS3* and *MEL1*) are only activated in the Y2HGold Yeast strain if the proteins interact and bind to the GAL4 responsive promotor. If the proteins do not interact there is no transcription of the reporter genes.

3.1.1 Construction of DNA-BD and AD gene fusion

Putative Nox interacting proteins used for the yeast two-hybrid screening can be found in **Table 2.2**. We also utilised plasmids previously constructed in the Talbot lab including *MEP1* and *MEP3* (Yan and Talbot, unpublished), *NOX1*, *PKC1* (Penn, 2010), *NOXR*, in the pGBKT7 vector and *NOXR, RAC1* (Ryder and Talbot, unpublished) and *NOXD* (Galhano et al., 2017) in the PGADT7 vector. Primers were designed with a 16 base pair homologous region corresponding to either the bait or prey vector depicted in **Figure 2.1a** to allow correct ligation into the vector using infusion based cloning (**Table 2.2**). Initially 8 hours post inoculation RNA from appressoria was used to generate cDNA to amplify the cDNA inserts, however amplification was unsuccessful (**Figure 3.2b**). Using RNA-seq data for a time course of infection-related development of *M. oryzae*, we could confirm, 0 hpi data showed the highest expression for the genes in this study. Therefore, Guy11 conidial RNA was used to generate the template cDNA to amplify the cDNA inserts. Once the inserts underwent gel purification they were ligated into

the multiple cloning site of the appropriate linearized vectors, double-digested with *Bam*HI and *Eco*RI restriction endonucleases (**Figure 3.2c**). Ligated vectors found in **Figure 3.3b** were transformed into competent *Escherichia coli* for continuous amplification of recombinant vectors and transferred to vancomycin or ampicillin antibiotic infused medium to select for positive transformants. To determine whether the cloning of the cDNA insert into the desired vector was successful, colony PCR assays using gene-specific primers was performed using SapphireAMP (**Figure 3.2d)**. For each construct multiple colonies were tested. Positive colonies were grown and recombinant vectors were extracted and purified as described in Chapter 2.4.3. Positive clones were also confirmed by restriction digest with the restriction enzymes *Eco*RI and *Bam*HI to release the original cDNA insert (**Figure 3.2e)**. Vectors were also independently verified by DNA sequencing (Eurofins MWG Operon) to ensure the alignment of in frame fusion of the gene to the BD and AD domains in the pGBKT7 and pGADT7 respectively. Positive vectors were transformed into YeastGold (Clontech Laboratories, Inc.).

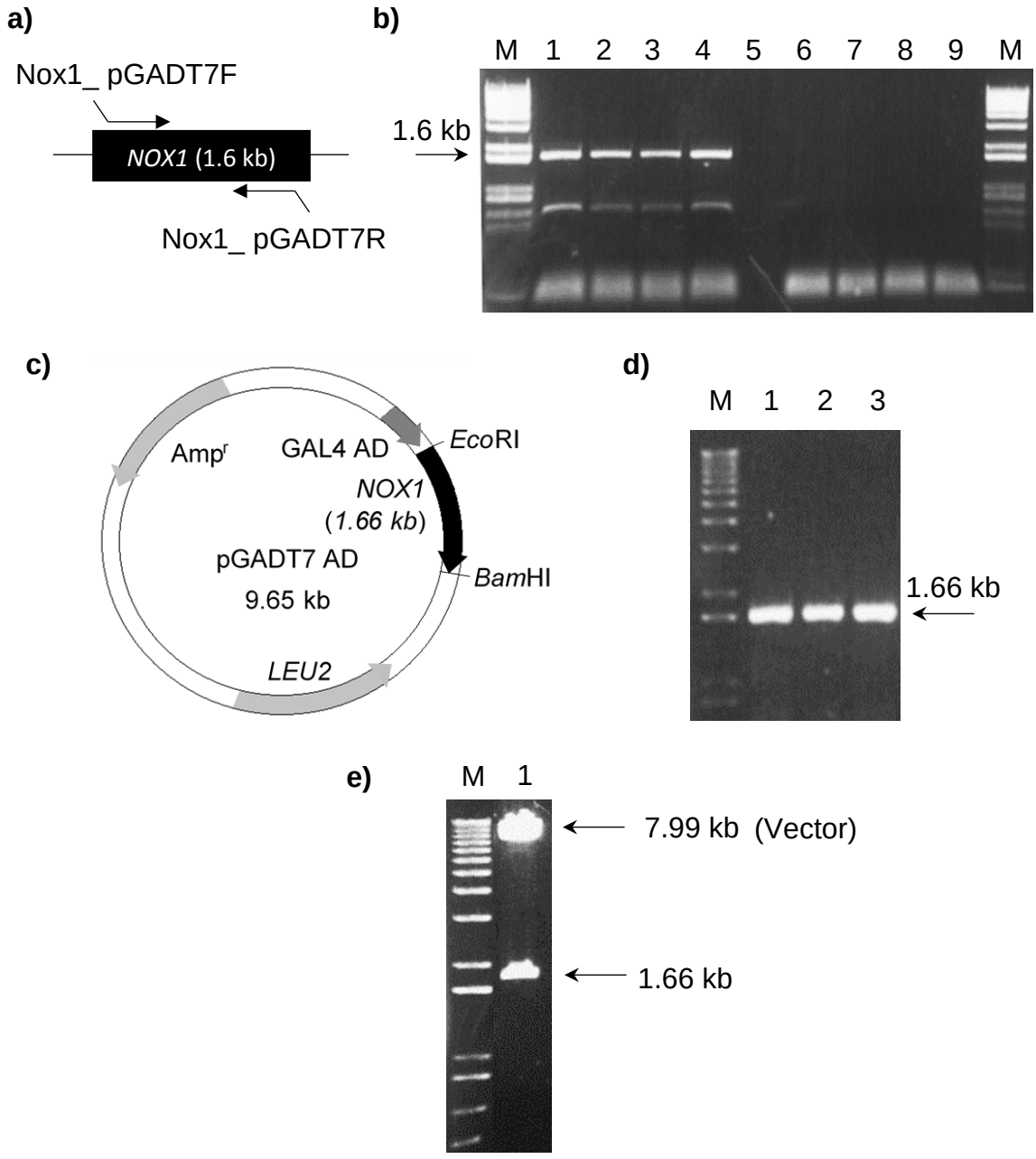

Figure 3.2 Systematic representation of the cloning strategy used for yeast two-hybrid vector construction.

a) Amplification of *NOX1* cDNA using *NOX1* specific primers with flanking regions corresponding to pGADT7 vector **b)** M (Marker); Lane 1-4 (*NOX1*-prey insert amplicon using conidial cDNA template), Lane 6-9 (failed amplification using 8 hour post inoculation cDNA template). Expected band size: 1.6 kb. **c)** The *NOX1* amplicon was ligated into digested pGADT7 vector resulting in the recombinant vector. **d)** Lane 1-3 (positive colony PCR of transformed competent *Escherichia coli* containing the construct). **e)** Lane 1 (extracted and purified recombinant plasmid confirmed using restriction digest with *Eco*RI and *Bam*HI).

3.1.2 Autoactivation and toxicity testing

Before testing putative Nox proteins control experiments were performed to confirm that constructs do not autoactivate the reporter genes autonomously or cause toxicity. All recombinant vectors were individually transformed into the YeastGold strain and plated on minimal SD medium in the absence of leucine (SD/-Leu) and tryptophan (SD/-Trp). Clones containing pGBKT7 vectors only grew on –Leu plates and clones containing pGADT7 vectors only grew on –Trp plates. No evidence of autoactivation or toxicity was observed as all clones were able to grow on appropriate medium. An example of this is shown in **Figure 3.3** for the pGADT7-*NOX1* recombinant vector. This reduces the possibility of false positives and false negatives in future experiments.

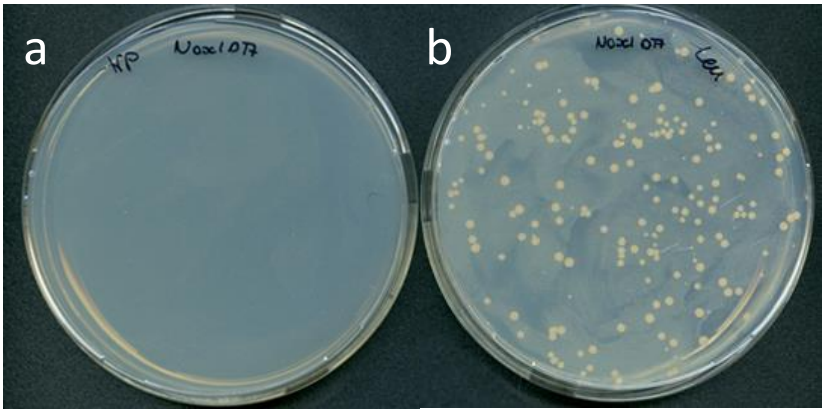

Figure 3.3 Autoactivation and toxicity test of transformed YeastGold containing the recombinant vector pGADT7 with ligated *NOX1.*

a) No growth of yeast transformants on SD/-Trp medium. **b)** Growth of single colony yeast transformants on SD/-Leu medium. Individually transformed constructs did not independently activate reporter genes or cause toxicity in yeast.

3.1.3 Determining the physical interactions between putative Nox proteins using yeast two hybrid

The yeast host strain (YeastGold, Clontech) was transformed using all the possible combinations of putative Nox complex components into the bait and prey vectors. Positive control (pGBKT7-53/pGADT7-T) supplied by Clontech uses a large T-antigen and murine p53 which are known to interact in a yeast two hybrid study. Negative control (pGBKT7/pGADT7) which are empty vectors and will not interact were used and an additional negative control, the metalloproteases *MEP1* and *MEP3* (Yan and Talbot, unpublished) were tested against putative proteins as well. The metalloproteases were identified as candidate effector proteins and primarily expressed and function *in planta*, and therefore are unlikely to interact with the Nox complex.

To select diploid cells containing both recombinant vectors, single colonies were isolated from SD/-Leu/-Trp agar plates for each combination. 10 randomly selected colonies were grown on medium stringency medium (SD/-His-Leu-Trp supplemented with X-α-Gal) and high stringency medium (SD/-Ade-His-Leu-Trp supplemented with X-α-Gal). These selection mediums were used as the yeast host strain is unable to synthesis histidine and adenine. However, when the bait and prey proteins positively interact, the *HIS3* and *ADE2* genes are expressed and the yeast cells are then able to grown on medium lacking histidine and adenine. The high stringency medium also contains X-α-Gal which turns the yeast colony blue if the two proteins interact causing the reporter gene to be expressed (*MEL1*). If the yeast able to grow on SD/-Leu/-Trp agar plates but not on the selection medium this indicated that the proteins did not interact meaning the reporter genes were not expressed and therefore was considered a negative interaction. To reduce false positives and display the strongest positive

interactions the high stringency media was used as it needs all reporter genes to be expressed to allow yeast growth to occur.

Dilutions of colonies were completed to avoid false positives and incubated at 30 °C for 4-5 days, seen in **Figure 3.4**. Colonies observed on medium and high stringency medium were considered as positive protein-protein interactions (**Table 3.1)**, with interactions only observed on medium considered transient interactions. An interaction map was produced to show the putative molecular organisation of the Nox complex components, which displays the medium stringency results as well as the high stringency results gathered in this study (**Figure 3.5**). Using the high stringency positive interactions from this study, presented in **Table 3.1**, a model of Nox1 and Nox2 complexes was constructed (**Figure 4.1**).

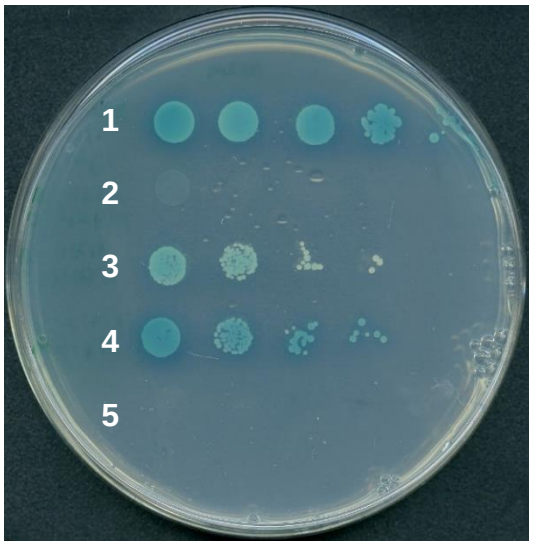

DNA-BD/AD

1 pGBKT7-53/pGADT7-T

2 pGBKT7/pGADT7

3 *BEM1/CDC42*

4 *BEM1/CDC24*

5 *PLS1/NOX1*

Figure 3.4 A Yeast two-hybrid assay with 10x dilutions for each DNA-BD/AD combination.

YeastGold was co-transformed with a pair of DNA-BD and AD vectors in different combinations. Yeast two-hybrid transformants and four 10x dilutions were plated in a single row on high stringency medium with X-α-Gal (SD/-Ade-His-Leu-Trp + X-α-Gal). Plates were inverted and incubated for 30°C for 4-5 days. Positive and negative controls were plated, row 1 and 2 respectively. A positive result with all four reporter genes activated is seen for row 3 and 4. A negative result was seen for row 5.

Table 3.1 High stringency Positive Protein-protein Interactions.

DNA-BD	AD	-Leu/-Trp	High Stringency + X- α-Gal
pGBKT7	pGADT7		
pGBKT7-53	pGADT7-T		
BEM1	*NOX1*		
	NOX2		
	PLS1		
	CDC24		
	CDC42		
	RAC1		
	NOXD		
	NOXR		
CDC24	*CHM1*		
	CDC42		
	BEM1		
	NOXR		
NOXR	*CDC24*		
	RAC1		
CHM1	*BEM1*		
MAS1			
PKC			
RAC1	*NOXR*		
NOX3	*PLS1*		

Table 3.1 High stringency Positive Protein-protein Interactions.

YeastGold (Clontech Laboratories) was co-transformed with a bait and prey vector. Positive and negative controls were included pGBKT7-53/pGADT7-T and pGBKT7/pGADT7 respectively. Transformants were plated onto high stringency medium with X-α-Gal (SD/-Ade-His-Leu-Trp + X-α-Gal), inverted and incubated at 30 °C for 4-5 days. Colonies will only grow on high stringency medium with X-α-Gal if the three nutritional reporters are expressed and colonies will turn blue if all 4 reporter genes are expressed. If all four reporter genes are expressed, this is counted as a strong positive putative protein-protein interaction.

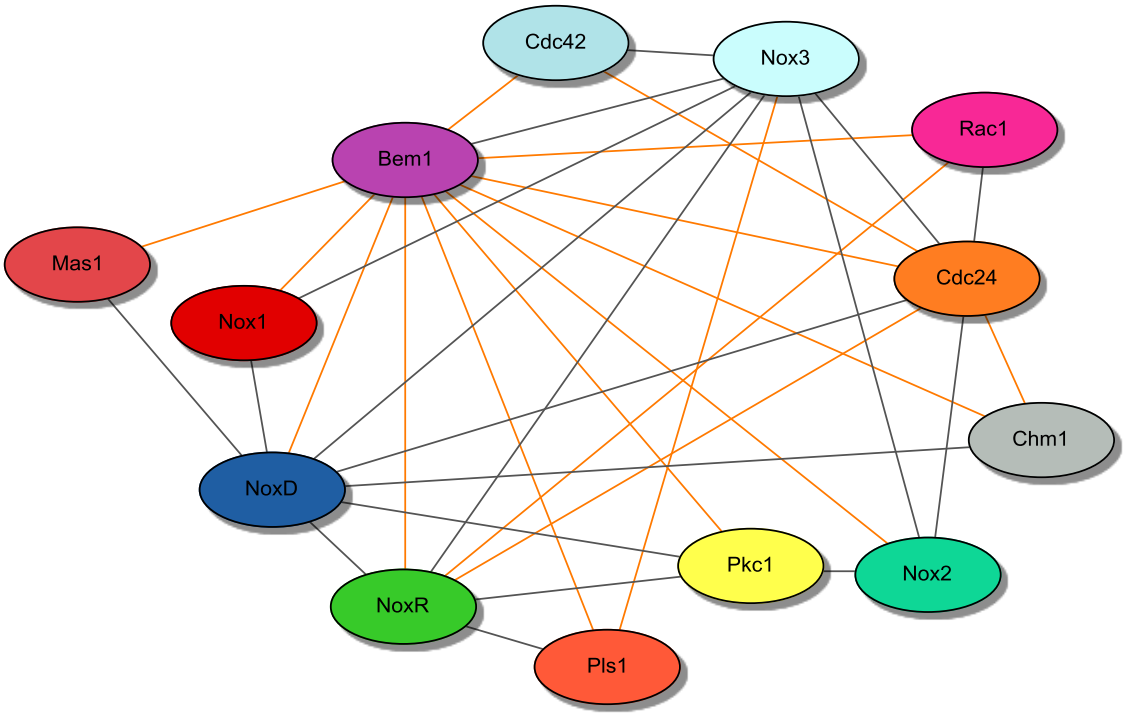

Figure 3.5 Protein-Protein Interaction map between putative Nox complex components.

A network of individual physical interactions of putative Nox complex components identified by yeast-two hybrid assays. Each node represents a protein and each link an interaction between two proteins. Orange links represent strong interactions observed on high stringency medium (SD/-Ade-His-Leu-Trp) and grey links represent weaker interactions observed on medium stringency medium (SD/-His-Leu-Trp).

3.2 Functional analysis of a *Δpls1* mutant of *M. oryzae*

3.2.1 Generation of a *Δpls1* by split gene replacement in *M. oryzae*

To characterise *PLS1,* an independent *Δpls1* mutant was generated to compare with other previously generated mutants in different background *M. oryzae* strains (Clergeot et al., 2001). The split marker gene deletion method was used to replace the open reading frame (ORF) of *PLS1* with a hygromycin phosphotransferase cassette marker (Millipore corp) (**Figure 3.6**). Left and right adjacent flanking regions (800 bp) of the *PLS1* ORF were amplified. Primers used, found in **Table 2.3,** were designed with overhang sequence complementary to the M13F and M13R (Primers: 50.1_PLS1F/50.1_PLS1R, 30.1_PLS1F/30.1PLS1R). Two halves of the hygromycin phosphotransferase cassette were amplified (Primers: M13F/HY split, YG split/M13R). The second round of PCR fused the left flanking amplicon to the HY amplicon and the right flanking amplicon with the YG amplicon. This produced two fragments that were transformed in a Guy11 background and by homologous recombination the ORF of *PLS1* was replaced with the hygromycin resistant gene.

3.2.2 Confirmation of a *ΔPLS1* transformant of *M. oryzae* using southern blot

Transformants were picked under selection of hygromycin B. A total of 26 were isolated. Genomic extraction of the transformants and digestion overnight at 37 °C with *Fsp*I was performed before separation by size on a gel (**Figure 3.7a**). The gel was then blotted and transferred to an N-Hybond membrane (Amersham). This was then probed using the 800 bp left flanking fragment (*Pls1* LF). Hybridisation of the probe to genomic DNA from the wildtype *M. oryzae* strain Guy11 resulted in a band at 1.6 kb and to transformants DNA a band at 4 kb. One positive transformant, T2, was confirmed (**Figure 3.7b**).

3.2.3 *M. oryzae ΔPLS1* is a non-pathogenic mutant

To determine the pathogenicity of Δpls1 compared to the wildtype Guy11, 14 day old CO-39 (*Oryzae sativa*) seedlings were sprayed with a conidial suspension of $1x10^4$/ml. These plants were incubated for 5 days before harvesting and analysis of the leaves (**Figure 3.8a**). Droplet leaf sheath assays were also performed in parallel using a conidial suspension of $1x10^5$/ml and incubated for 4-5 days (**Figure 3.8b**). To control discrepancy between leaves a droplet of Guy11 conidial suspension was placed on each leaf sheath. *Δpls1* had no visible signs of infection with either the spray or droplet inoculated assays, suggesting that *Δpls1* is non-pathogenic on rice plants.

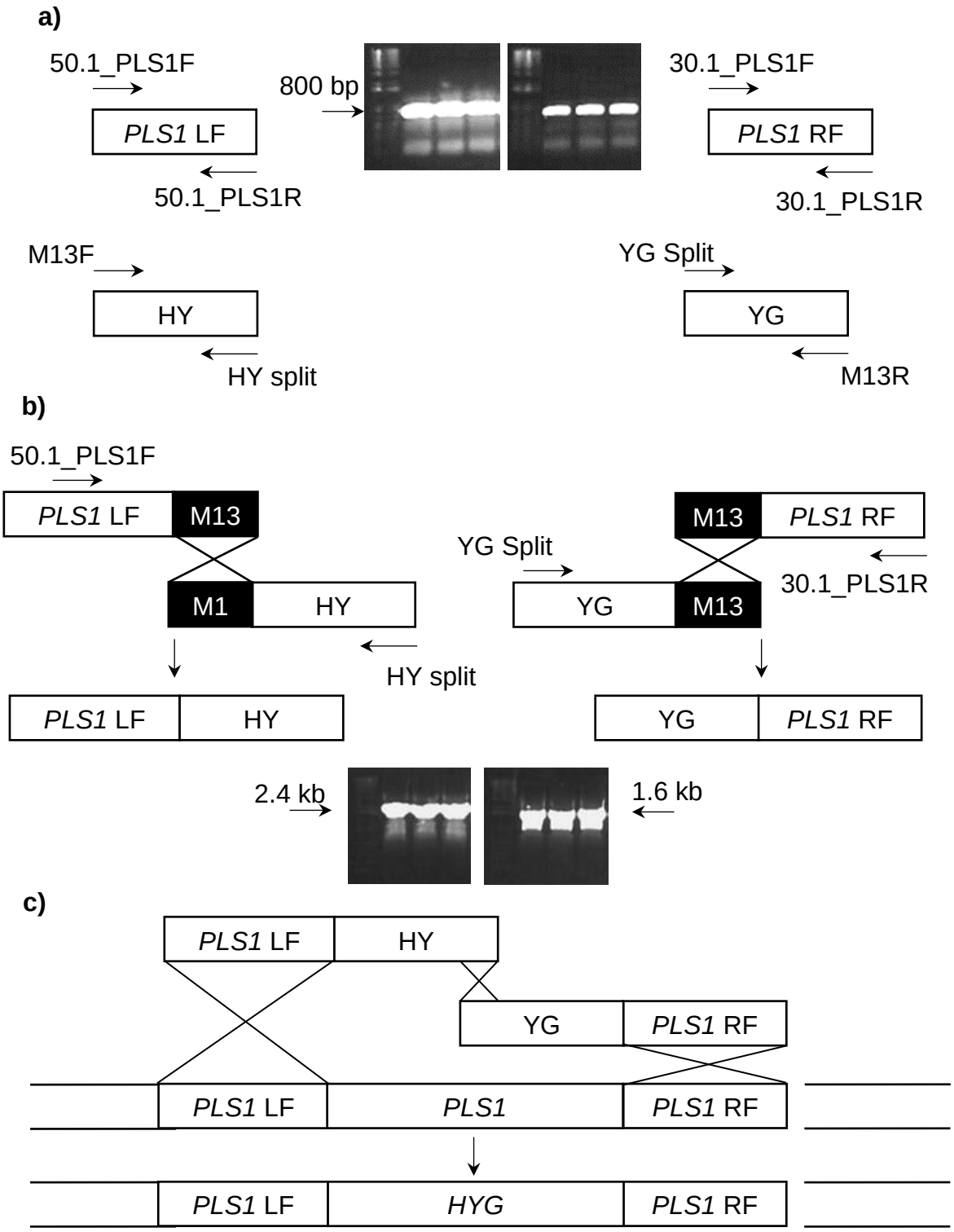

Figure 3.6 Schematic representation of the split marker gene method.

a) Amplification of the right and left 800 bp flanking regions adjacent to the *PLS1* open reading frame (ORF) and each half of the hygromycin cassette. **b)** Two PCR amplifications fuse the flanking regions to HY and YG fragments of the hygromycin phosphotransferase cassette. **c)** Transformation of the two fragments results in homologous recombination replacing *PLS1* ORF with the hygromycin phosphotransferase cassette.

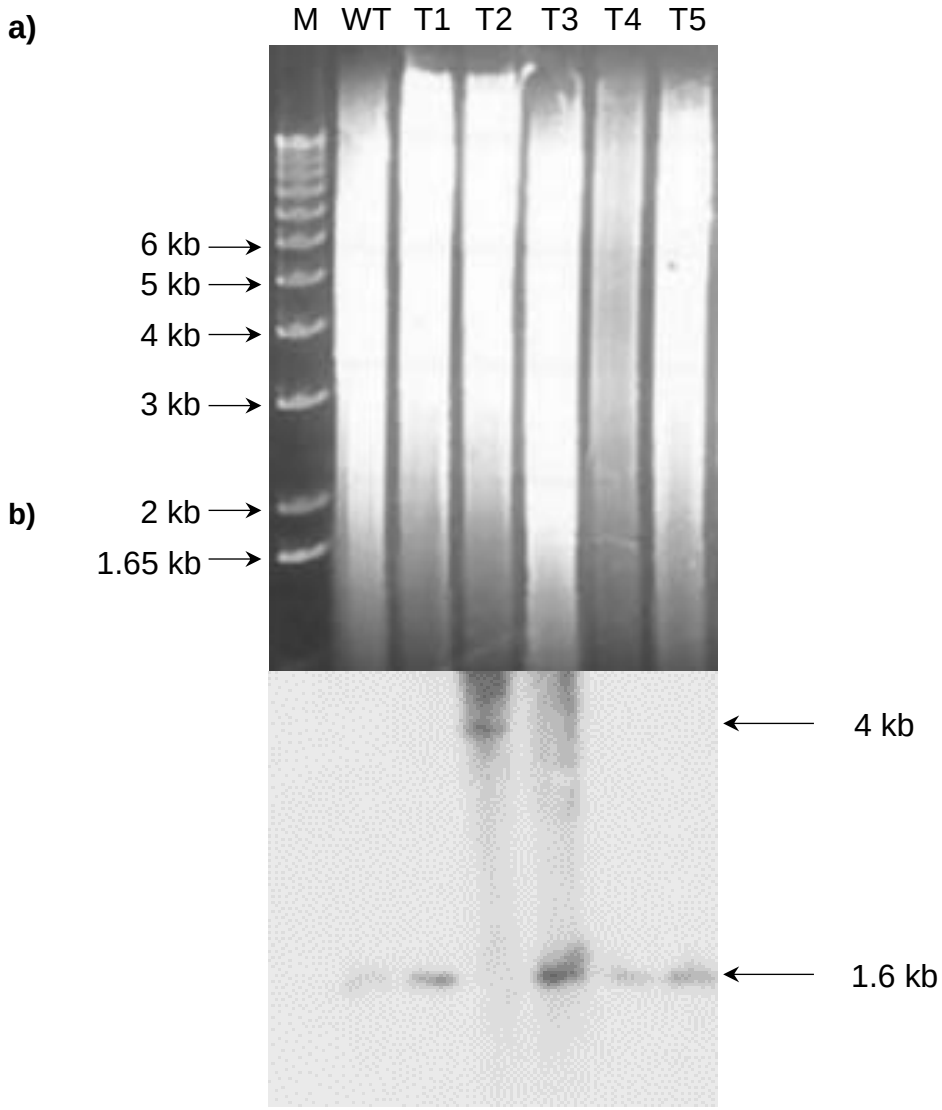

Figure 3.7 Southern analysis of putative *Δpls1* transformants.

Analysis of potential *Δpls1* transformants was completed using Southern blotting. **a)** M (Marker); Genomic DNA of transformants was extracted from transformants and digested using *Fsp*I. **b)** The Southern blot was probed with the 800 bp left flanking upstream region (*PLS1* LF). The probe hybridises with wildtype DNA to produce a fragment of 1.6 kb and for transformant DNA at 4 kb. The Southern blot provided evidence of a targeted gene replacement mutant for T2.

Figure 3.8 The *Δpls1* mutant is non-pathogenic.

a) Three week-old seedlings of the blast susceptible rice cultivar 30-39 were spray inoculated with wild type Guy11 and the mutant *Δpls1* at a density of 5 x 10^4 spores ml^{-1} and incubated for 5 days. **b)** Drop inoculated onto 14 day old CO-39 with a control Guy11 droplet at the bottom of each leaf sheath. Leaf sheaths were incubated for 5 days post inoculation before visualisation.

4. Discussion

The yeast two-hybrid assays revealed putative physically interacting proteins of the Nox complex and using the data collected a model was generated of the putative Nox1 and Nox2 complexes (**Figure 4.1**). The three Nox flavoenzymes in *M. oryzae* have different physical interactions with the putative Nox complex components used in the yeast two-hybrid assay. As previously reported in *B. cinerea,* Nox1 and the orthologue of $p22^{phox}$, NoxD physically interact in *M. oryzae* (Siegmund et al., 2015). In comparison Nox2 does not interact with NoxD but with Pkc1 and Cdc24 unlike Nox1. It is unknown why the ROS burst generated by NOX is necessary for infection and the specific roles for Nox1 and Nox2 in *M. oryzae*. I conclude that Nox1 and Nox2 have different interaction profiles during the yeast two-hybrid analysis with putative Nox complex components. These profiles could, in conjunction with their different mutant phenotypes, be used to understand their roles within appressorium formation and plant infection.

I have shown here that there is a physical interaction between Rac1 and proteins including Bem1, Cdc24 and NoxR. This supports previous research that states these components are required to form an active Nox complex during fungal morphogenesis and growth (Schürmann et al., 2013; Tanaka et al., 2012). As expected the study revealed that NoxR, the regulatory component, had a strong interaction with homologues of the yeast polarity proteins, Bem1 and Cdc24 previously reported in *Epichloë festucae* (Kawahara & Lambeth, 2007; Takemoto et al., 2011). Fungal Bem1 contains protein-protein interaction domains which would enable interactions with other proteins (Takemoto et al., 2011). In past studies the function of Bem1 has been described as a strong candidate for a scaffold protein not only in *M. oryzae* but in *C. purpurea* (Kawahara & Lambeth, 2007; Takemoto et al., 2011). In E. festucae it has been reported that Cdc24 is

the guanine-nucelotide exchange factor (GEF) for Rac1 and as Bem1 interacts with NoxR and Cdc24 it is likely that Bem1 facilitates the recruitment of NoxR-Cdc24 to the Nox complex (Takemoto et al., 2011). From the interactions recorded, Bem1 interacted with all putative Nox complex components reported in this study and strongly interacted with 11 out of 12, indicating that Bem1 is a scaffold protein for the Nox complex. The activation of the Nox complex requires the scaffold protein Bem1 to recruit NoxR and other Nox related components to the complex to activate Nox1/2 for ROS production to occur (Kawahara & Lambeth, 2007; Takemoto et al., 2011).

In this dissertation, I have provided evidence that Chm1 physically interacts with several Nox complex components including Bem1, Cdc24 and NoxD. *Δnox2* and *ΔnoxR* mutant phenotypes display a disorganised Chm1 and septin ring during penetration peg formation and has shown Chm1-GFP localisation to be a Nox2/R dependent process (Ryder et al., 2013). Taken with my results this suggests that Nox2 and NoxR have a role in Chm1 ring localisation and assembly through direct association with the multiple Nox complex components. The formation of the penetration peg is a septin-mediated F-actin dependent process and Chm1 is known to phosphorylate septins (Dagdas et al., 2012; Versele & Thorner, 2004). To conclude, activation of the Nox complex is associated with cytoskeleton remodelling for penetration peg formation during plant infection in *M. oryzae.*

Generation of a *Δpls1* mutant in a Guy11 background was used to compare results with previous studies. Using Guy11 in the targeted gene replacement of *Δpls1* instead of the 70-15 strain or *Magnaporthe grisea*, as seen in other studies, removes the unknown implications of using a genetically altered background strain therefore, increasing the validity of any analysis (Clergeot et al., 2001; Ryder et al., 2013). The resultant mutant showed the deletion of *PLS1* was not

essential to viability however, the leaf infection assays verify that *Δpls1* is non-pathogenic and is unable to cause infection on rice as found in *M. grisea* (Clergeot et al., 2001). *PLS1* has been suggested to have a direct role in the Nox complex functioning as a $p22^{phox}$ like protein (Lacaze et al., 2015). This is because NoxR, a $p22^{phox}$ homologue, and Nox1 which are known to interact and have similar mutant phenotypes, which is also seen with *Δpls1* and *Δnox2* mutants (Siegmund et al., 2015). My yeast two-hybrid results do not show an interaction between Pls1 and Nox2, however they do show an interaction with Pls1 and other Nox complex components, Bem1 and NoxR. To conclude, Pls1 is likely to be involved in Nox dependent septin-mediated F-actin cytoskeleton reorganisation for penetration peg formation.

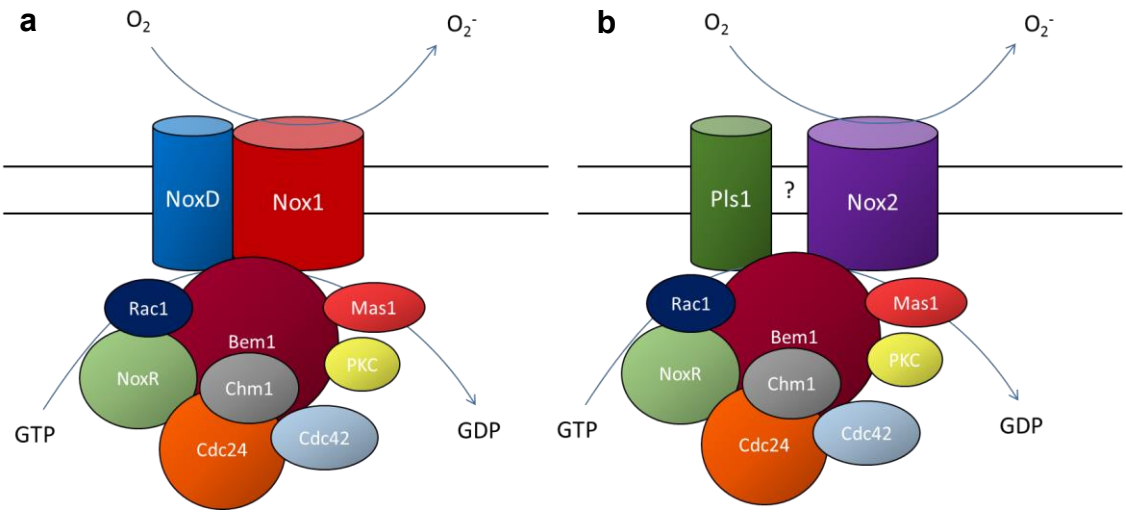

Figure 4.1 Proposed model depicting the Nox1 and Nox2 complex using yeast two-hybrid data.

Using yeast two-hybrid data collated from this study the following models have been proposed to depict the composition and components of the Nox complexes, **a)** *NOX1* and **b)** *NOX2*. Proteins are not to scale.

Future research should focus on the verification of the interactions reported in this study, to identify the assembly of the Nox complex and the differences between Nox1 and Nox2 complexes. My results showed few interactions for Nox1, Nox2 and Pls1 however, the yeast two-hybrid system has limited results regarding transmembrane proteins as protein-protein interactions must occur in the nucleus for the reporter gene to be activated and the transmembrane protein interactions may not be detected. To overcome these limitations a split-ubiquitin yeast two-hybrid system may be able to detect the interactions of insoluble membrane bound proteins (Johnsson & Varshavsky, 1994). Further research should also be carried out such as co-immunoprecipitation which would be able to determine and verify interacting proteins of the Nox complex from this study, using mass spectrometry (Rigaut et al., 1999). Surface plasmon resonance to establish the strength of each interaction temporally and label-free should also be considered in any future research (Schuck, 1997). These experiments should focus on Nox2 and Pls1 which are predicted to interact, with Pls1 acting with a similar activity as the mammalian adaptor protein, $p22^{phox}$ (Tudzynski et al., 2012). X-ray crystallography would be another method to verify the assembly of the complex and the interaction between Pls1 and Nox2.

Previous methods only show if proteins are able to interact however, identifying temporal variations and downstream effects of the Nox complex would be an important area of research as it may elucidate the mechanism of penetration peg formation and elongation into the host cell. Analysis using bimolecular fluorescence complementation *in vivo* would show when two proteins are interacting and therefore when Nox related proteins are recruited to the Nox complex for activation. This method would also be useful in determining if Pls1 and Nox2 interact directly or if there is an adaptor protein. If used in conjunction

with fluorescent tagging of cytoskeleton structures this would reveal when and which proteins are recruited to the complex during Nox activation to cause cytoskeleton remodelling with particular attention to Chm1, septins and F-actin.

The methods discussed above could be used with mutant phenotypes such as *ΔnoxR* and *Δbem1* to see the effect of other proteins recruited to the Nox complex and cytoskeleton abnormalities. Further work looking into the effect of *PLS1*, using the mutant generated in this study should localise Nox1/2 as well as other Nox complex components and cytoskeleton structures such as: F-actin, septin and Chm1 rings using green florescent protein tagging. This would determine whether the mutant has disorganised networks accounting for the non-pathogenic phenotype similar to the 70-15 mutant described previously (Ryder et al., 2013).

In summary, I have shown the Nox complexes of *M. oryzae* are mainly composed of at least 10 proteins in addition to Nox enzymes. The likely difference between the complexes is in the addition of the membrane-bound component such as Pls1 and NoxD although future work needs to be completed to verify this difference. Nox1, Nox2 and Nox3 have different interactions and I expect complexes will not be comprised of entirely the same proteins. I also generated a *Δpls1* mutant and this provides a resource to functionally characterise the role of a tetraspanin in *M. oryzae*.

5. Acknowledgements

I would like to thank my supervisor Nick Talbot for providing continual guidance and support, and all the members of Lab 301 in particular Lauren Ryder for all the help I have received.

6. Bibliography

Baldridge, C. W., & Gerard, R. W. (1933). The Extra Respiration of Phagocytosis. *American Journal of Physiology*, *103*, 235–236. Retrieved from www.physiology.org/journal/ajplegacy

Bhattacharya, R., & Mondal, H. (2017, March 4). Fungus sees wheat crops in Bengal go up in flames as govt controls its spread. *Hindustran Times*. Chapra, West Bengal. Retrieved from http://www.hindustantimes.com/india-news/fungus-sees-wheat-crops-in-bengal-go-up-in-flames-as-govt-controls-its-spread/story-ok3NRwnvzR3InZwFnmZcHL.html

Bourett, T. M., & Howard, R. J. (1990). In vitro development of penetration structures in the rice blast fungus Magnaporthe grisea. *Canadian Journal of Botany*, *68*(2), 329–342. https://doi.org/10.1139/b90-044

Callaway, E. (2016). Devastating wheat fungus appears in Asia for first time. *Nature News*, *532*, 421–422. https://doi.org/10.1038/532421a

Cano-Domínguez, N., Alvarez-Delfín, K., Hansberg, W., & Aguirre, J. (2008). NADPH oxidases NOX-1 and NOX-2 require the regulatory subunit NOR-1 to control cell differentiation and growth in Neurospora crassa. *Eukaryotic Cell*, *7*(8), 1352–61. https://doi.org/10.1128/EC.00137-08

Chen, J., Zheng, W., Zheng, S., Zhang, D., Sang, W., Chen, X., Li, G., Lu, G., & Wang, Z. (2008). Rac1 Is Required for Pathogenicity and Chm1-Dependent Conidiogenesis in Rice Fungal Pathogen Magnaporthe grisea. *PLOS Pathogens*, *4*(11), 1–16. https://doi.org/10.1371/journal.ppat.1000202

Clergeot, P.-H., Gourgues, M., Cots, J., Laurans, F., Latorse, M.-P., Pépin, R.,

Tharreau, D., Notteghem, J.-L., & Lebrun, M.-H. (2001). PLS1, a gene encoding a tetraspanin-like protein, is required for penetration of rice leaf by the fungal pathogen Magnaporthe grisea. *Proceedings of the National Academy of Sciences of the United States of America*, *98*(12), 6963–6968. Retrieved from http://www.pnas.org/content/98/12/6963.full.pdf

Couch, B. C., Fudal, I., Lebrun, M.-H., Tharreau, D., Valent, B., Kim, P. Van, Nottéghem, J.-L., & Kohn, L. M. (2005). Origins of Host-Specific Populations of the Blast Pathogen Magnaporthe oryzae in Crop Domestication With Subsequent Expansion of Pandemic Clones on Rice and Weeds of Rice. *The Genetic Society of America*, *170*(2), 613–630. https://doi.org/10.1534/genetics.105.041780

Cross, A. R., & Segal, A. W. (2004). The NADPH oxidase of professional phagocytes-prototype of the NOX electron transport chain systems. *Biochimica et Biophysica Acta*, *1657*, 1–22. https://doi.org/10.1016/j.bbabio.2004.03.008

Dagdas, Y. F., Yoshino, K., Dagdas, G., Ryder, L. S., Bielska, E., Steinberg, G., & Talbott, N. J. (2012). Septin-Mediated Plant Cell Invasion by the Rice Blast Fungus, Magnaporthe oryzae. *Science*, *336*(6088), 1590–1595. https://doi.org/10.1073/PNAS.0901477106

Das, S. (2017, March 6). “Wheat blast” disease enters India from Bangladesh, ICAR official says damage contained. *The Financial Express*. New Delhi. Retrieved from http://www.financialexpress.com/india-news/wheat-blast-disease-enters-india-from-bangladesh-icar-official-says-damage-contained/576247/

de Jong, J., McCormack, B., Smirnoff, N., & Talbot, N. (1997). Glycerol

generates turgor in rice blast. *Nature*, *389*(September), 244–245. https://doi.org/10.1038/38418

Dean, R. A. (1997). Signal Pathways and Apressorium Morphogenesis. *Annu. Rev. Phytopathol*, *35*, 211–34. Retrieved from http://www.annualreviews.org/doi/pdf/10.1146/annurev.phyto.35.1.211

Dean, R., Van Kan, J. A. L., Pretorius, Z. A., Hammond-kosack, K. E., Di Pietro, A., Spanu, P. D., Rudd, J. J., Dickman, M., Kahmann, R., Ellis, J., & Foster, G. D. (2012). The Top 10 fungal pathogens in molecular plant pathology. *Molecular Plant Pathology*, 1–17. https://doi.org/10.1111/J.1364-3703.2011.00783.X

Ebbole, D. J. (2007). Magnaporthe as a Model for Understanding Host-Pathogen Interactions. *Annu. Rev. Phytopathol.*, *45*, 436–456. https://doi.org/10.1146/annurev.phyto.45.062806.094346

Egan, M. J., Wang, Z., Jones, M. A., Smirnoff, N., & Talbot, N. J. (2007). Generation of reactive oxygen species by fungal NADPH oxidases is required for rice blast disease. *Proceedings of the National Academy of Sciences of the United States of America*, *104*(28), 11.

Foreman, J., Demidchik, V., Bothwell, J. H. F., Mylona, P., Miedema, H., Torres, M. A., Linstead, P., Costa, S., Brownlee, C., Jones, J. D. G., Davies, J. M., & Dolan, L. (2003). Reactive oxygen species produced by NADPH oxidase regulate plant cell growth. *Nature*, *422*(6930), 442–446. https://doi.org/10.1038/nature01485

Galhano, R., Illana, A., Ryder, L. S., Rodríguez-Romero, J., Demuez, M., Badaruddin, M., Martinez-Rocha, A. L., Soanes, D. M., Studholme, D. J.,

Talbot, N. J., & Sesma, A. (2017). Tpc1 is an important Zn(II)2Cys6 transcriptional regulator required for polarized growth and virulence in the rice blast fungus. *PLOS Pathogens*, *13*(7), e1006516. https://doi.org/10.1371/journal.ppat.1006516

Gourgues, M., Brunet-Simon, A., Lebrun, M.-H., & Levis, C. (2004). The tetraspanin BcPls1 is required for appressorium-mediated penetration of Botrytis cinerea into host plant leaves. *Molecular Microbiology*, *51*(3), 619–29. Retrieved from http://www.ncbi.nlm.nih.gov/pubmed/14731267

Hamer, J. E., Howard, R. J., Chumley, F. G., & Valent, B. (1988). A Mechanism for Surface Attachment in Spores of a Plant Pathogenic Fungus. *Science*, *239*(4837), 288–290. https://doi.org/10.1126/science.239.4837.288

Holmes, B., Page, A., & Good, R. (1967). Studies of the Metabolic Activity of Leukocytes from Patients with a Genetic Abnormality of Phagocytic Function. *Journal of Clinical Investigation*, *46*(9), 1422–1432. Retrieved from https://dm5migu4zj3pb.cloudfront.net/manuscripts/105000/105634/JCI67105634.pdf

Howard, R. J., Ferrari, M. A., Roach, D. H., & Money, N. P. (1991). Penetration of hard substrates by a fungus employing enormous turgor pressures. *Proceedings of the National Academy of Sciences*, *88*(24), 11281–11284. https://doi.org/10.1073/pnas.88.24.11281

Islam, M. T., Croll, D., Gladieux, P., Soanes, D. M., Persoons, A., Bhattacharjee, P., Hossain, M. S., Gupta, D. R., Rahman, M. M., Mahboob, M. G., Cook, N., Salam, M. U., Surovy, M. Z., Sancho, V. B., Maciel, J. L. N., NhaniJúnior, A., Castroagudín, V. L., Reges, J. T. de A., Ceresini, P. C.,

Ravel, S., Kellner, R., Fournier, E., Tharreau, D., Lebrun, M.-H., McDonald, B. A., Stitt, T., Swan, D., Talbot, N. J., Saunders, D. G. O., Win, J., & Kamoun, S. (2016). Emergence of wheat blast in Bangladesh was caused by a South American lineage of Magnaporthe oryzae. *BMC Biology*, *14*(1), 84. https://doi.org/10.1186/s12915-016-0309-7

Johnsson, N., & Varshavsky, A. (1994). Split ubiquitin as a sensor of protein interactions in vivo, *91*, 10340–10344. Retrieved from http://www.pnas.org/content/91/22/10340.full.pdf

Kankanala, P., Czymmek, K., & Valent, B. (2007). Roles for Rice Membrane Dynamics and Plasmodesmata during Biotrophic Invasion by the Blast Fungus. *The Plant Cell*, *19*(2), 706–724. https://doi.org/10.1105/tpc.106.046300

Kawahara, T., & Lambeth, J. D. (2007). Molecular evolution of Phox-related regulatory subunits for NADPH oxidase enzymes. *BMC Evolutionary Biology*, *7*(1), 178. https://doi.org/10.1186/1471-2148-7-178

Kershaw, M. J., & Talbot, N. J. (2009). Genome-wide functional analysis reveals that infection-associated fungal autophagy is necessary for rice blast disease. *Proceedings of the National Academy of Sciences of the United States of America*, *106*(37), 15967–72. https://doi.org/10.1073/pnas.0901477106

Kohli, M. M., Mehta, Y. R., Guzman, E., De Viedma, L., & Cubilla, L. E. (2010). *Pyricularia Blast-a Threat to Wheat Cultivation*. Retrieved from https://www.agriculturejournals.cz/publicFiles/48968.pdf

Lacaze, I., Lalucque, H., Siegmund, U., Silar, P., & Brun, S. (2015).

Identification of NoxD/Pro41 as the homologue of the p22 ^{phox} NADPH oxidase subunit in fungi. *Molecular Microbiology*, *95*(6), 1006–1024. https://doi.org/10.1111/mmi.12876

Lam, G. Y., Huang, J., & Brumell, J. H. (2010). The many roles of NOX2 NADPH oxidase-derived ROS in immunity. *Seminars in Immunopathology*, *32*, 415–430. https://doi.org/10.1007/s00281-010-0221-0

Lambeth, J. D. (2004). NOX enzymes and the biology of reactive oxygen. *Nature Reviews Immunology*, *4*(3), 181–189. https://doi.org/10.1038/nri1312

Lambou, K., Malagnac, F., Barbisan, C., Tharreau, D., Lebrun, M.-H., & Silar, P. (2008). The crucial role of the Pls1 tetraspanin during ascospore germination in Podospora anserina provides an example of the convergent evolution of morphogenetic processes in fungal plant pathogens and saprobes. *Eukaryotic Cell*, *7*(10), 1809–18. https://doi.org/10.1128/EC.00149-08

Lara-Ortíz, T., Riveros-Rosas, H., & Aguirre, J. (2003). Reactive oxygen species generated by microbial NADPH oxidase NoxA regulate sexual development in Aspergillus nidulans. *Molecular Microbiology*, *50*(4), 1241–1255. https://doi.org/10.1046/j.1365-2958.2003.03800.x

Malagnac, F., Lalucque, H., Lepè, G., & Silar, P. (2004). Two NADPH oxidase isoforms are required for sexual reproduction and ascospore germination in the filamentous fungus Podospora anserina. *Fungal Genetics and Biology*, *41*, 982–997. https://doi.org/10.1016/j.fgb.2004.07.008

Martin-urdiroz, M., Oses-ruiz, M., Ryder, L. S., & Talbot, N. J. (2015).

Investigating the biology of plant infection by the rice blast fungus Magnaporthe oryzae. *Fungal Genetics and Biology*, *90*, 1087–1845. https://doi.org/10.1016/j.fgb.2015.12.009

Osés Ruiz, M., & Talbot, N. J. (2017). Cell cycle-dependent regulation of plant infection by the rice blast fungus Magnaporthe oryzae. *Communicative & Integrative Biology*, *0*(0), 1–6. https://doi.org/10.1080/19420889.2017.1372067

Penn, T. J. (2010). *Investigating the Role of Protein Kinase C in Magnaporthe oryzae*. University of Exeter.

Reeves, E. P., Lu, H., Jacobs, H. L., Messina, C. G. M., Bolsover, S., Gabellak, G., Potma, E. O., Warley, A., Rgen Roes, J. È., & Segal, A. W. (2002). Killing activity of neutrophils is mediated through activation of proteases by K + flux. *Nature*, *416*, 291–297. Retrieved from www.nature.com

Rigaut, G., Shevchenko, A., Rutz, B., Wilm, M., Mann, M., & Séraphin, B. (1999). A generic protein purification method for protein complex characterization and proteome exploration. *Nature Biotechnology*, *17*(10), 1030–1032. https://doi.org/10.1038/13732

Ryder, L. S., Dagdas, Y. F., Mentlak, T. A., Kershaw, M. J., Thornton, C. R., Schuster, M., Chen, J., Wang, Z., & Talbot, N. J. (2013). NADPH oxidases regulate septin-mediated cytoskeletal remodeling during plant infection by the rice blast fungus. *Proceedings of the National Academy of Sciences of the United States of America*, *110*(8), 3179–84. https://doi.org/10.1073/pnas.1217470110

Sambrook, J., Fritsch, F. E., & Maniatis, T. (1989). Molecular cloning: A

laboratory manual. *Cold Harbor Laboratory Press*.

Sbarra, A. J., & Karnovskyi, M. L. (1959). The Biochemical Basis of Phagocytosis. *Journal of Biol Chem*, *234*(6), 1355–1362. Retrieved from http://www.jbc.org/

Schuck, P. (1997). Use of surface plasmon resonance to probe the equilibrium and dynamic aspects of interactions between biological macromolecules. *Annual Review of Biophysics and Biomolecular Structure*, *26*(1), 541–566. https://doi.org/10.1146/annurev.biophys.26.1.541

Schürmann, J., Buttermann, D., Herrmann, A., Giesbert, S., & Tudzynski, P. (2013). Molecular Characterization of the NADPH Oxidase Complex in the Ergot Fungus Claviceps purpurea: CpNox2 and CpPls1 Are Important for a Balanced Host-Pathogen Interaction. *Molecular Plant-Microbe Interactions*, *26*(10), 1151–1164. https://doi.org/10.1094/MPMI-03-13-0064-R

Seebold, K. W., Datnoff, L. E., Correa-Victoria, F. J., Kucharek, T. A., & Snyder, G. H. (2004). Effects of Silicon and Fungicides on the Control of Leaf and Neck Blast in Upland Rice. *Plant Disease*, *88*(3), 253–258. https://doi.org/10.1094/PDIS.2004.88.3.253

Segal, A. W. (2005). How Neutrophils Kill Microbes. *Annu. Rev. Immunol*, *23*, 197–223. https://doi.org/10.1146/annurev.immunol.23.021704.115653

Segal, A. W., & Jones, O. T. G. (1978). Novel cytochrome b system in phagocytic vacuoles of human granulocytes. *Nature*, *276*(5687), 515–517. https://doi.org/10.1038/276515a0

Siegmund, U., Heller, J., van Kan, J. A. L., & Tudzynski, P. (2013). The NADPH Oxidase Complexes in Botrytis cinerea: Evidence for a Close Association

with the ER and the Tetraspanin Pls1. *PLoS ONE*, *8*(2), e55879. https://doi.org/10.1371/journal.pone.0055879

Siegmund, U., Marschall, R., & Tudzynski, P. (2015). BcNoxD, a putative ER protein, is a new component of the NADPH oxidase complex in *B otrytis cinerea*. *Molecular Microbiology*, *95*(6), 988–1005. https://doi.org/10.1111/mmi.12869

Skamnioti, P., & Gurr, S. J. (2009). Against the grain: safeguarding rice from rice blast disease. *Trends in Biotechnology*, *27*(3), 141–150. https://doi.org/10.1016/j.tibtech.2008.12.002

Strange, R. N., & Scott, P. R. (2005). Plant Disease: A Threat to Global Food Security. *Annual Review of Phytopathology*, *43*(1), 83–116. https://doi.org/10.1146/annurev.phyto.43.113004.133839

Sumimoto, H., Miyano, K., & Takeya, R. (2005). Molecular composition and regulation of the Nox family NAD(P)H oxidases. *Biochemical and Biophysical Research Communications*, *338*(1), 677–686. https://doi.org/10.1016/J.BBRC.2005.08.210

Suzuki, N., Miller, G., Morales, J., Shulaev, V., Torres, M. A., & Mittler, R. (2011). Respiratory burst oxidases: the engines of ROS signaling. *Current Opinion in Plant Biology*, *14*(6), 691–699. https://doi.org/10.1016/J.PBI.2011.07.014

Takemoto, D., Kamakura, S., Saikia, S., Becker, Y., Wrenn, R., Tanaka, A., Sumimoto, H., & Scott, B. (2011). Polarity proteins Bem1 and Cdc24 are components of the filamentous fungal NADPH oxidase complex. *Proceedings of the National Academy of Sciences of the United States of*

America, *108*(7), 2861–6. https://doi.org/10.1073/pnas.1017309108

Takemoto, D., Tanaka, A., & Scott, B. (2007). NADPH oxidases in fungi: Diverse roles of reactive oxygen species in fungal cellular differentiation. *Fungal Genetics and Biology*, *44*(11), 1065–1076. https://doi.org/10.1016/j.fgb.2007.04.011

Talbot, N. J. (2003). On The Trail Of A Cereal Killer: Exploring the Biology of Magnaporthe grisea. *Annu. Rev. Microbiol*, *57*, 177–202. https://doi.org/10.1146/annurev.micro.57.030502.090957

Tanaka, A., Takemoto, D., Chujo, T., & Scott, B. (2012). Fungal endophytes of grasses. *Current Opinion in Plant Biology*, *15*(4), 462–468. https://doi.org/10.1016/j.pbi.2012.03.007

Torres, M. A., Dangl, J. L., & Jones, J. D. G. (2002). Arabidopsis gp91phox homologues AtrbohD and AtrbohF are required for accumulation of reactive oxygen intermediates in the plant defense response. *Proceedings of the National Academy of Sciences of the United States of America*, *99*(1), 517–22. https://doi.org/10.1073/pnas.012452499

Tudzynski, P., Heller, J., & Siegmund, U. (2012). Reactive oxygen species generation in fungal development and pathogenesis. *Current Opinion in Microbiology*, *15*(6), 653–659. https://doi.org/10.1016/j.mib.2012.10.002

United Nations, Department of Economic and Social Affairs, Population Division (2017). World Population Prospects: The 2017 Revision, K. F. and A. T. E. (2017). *United Nations*.

Valent, B., & Chumley, F. G. (1991). Molecular genetic analysis of the rice blast fungus, Magnaporthe grisea. *Annu. Rev. Phytopathol.*, *29*(1), 443–467.

Versele, M., & Thorner, J. (2004). Septin collar formation in budding yeast requires GTP binding and direct phosphorylation by the PAK, Cla4. *The Journal of Cell Biology*, *164*(5), 701–15. https://doi.org/10.1083/jcb.200312070

Wilson, R. A., & Talbot, N. J. (2009). Under pressure: investigating the biology of plant infection by Magnaporthe oryzae. *Nature Reviews Microbiology*, *7*(3), 185–195. https://doi.org/10.1038/nrmicro2032

Xue, C., Park, G., Choi, W., Zheng, L., Dean, R. A., & Xu, J. (2002). Two Novel Fungal Virulence Genes Specifically Expressed in Appressoria of the Rice Blast Fungus, *14*(September), 2107–2119. https://doi.org/10.1105/tpc.003426.pressorium

Yan, X., & Talbot, N. J. (2016). Investigating the cell biology of plant infection by the rice blast fungus Magnaporthe oryzae. *Current Opinion in Microbiology*, *34*, 147–153. https://doi.org/10.1016/j.mib.2016.10.001